The gut bacterial community potentiates *Clostridiodes difficile* infection severity.

Running title: Microbiota potentiates *Clostridioides difficile* infection severity

Nicholas A. Lesniak[1], Alyxandria M. Schubert[1], Kaitlyn Flynn[1], Jhansi L Leslie[1], Hamide Sinani[1], Ingrid L. Bergin[3], Vincent B Young[2], Patrick D. Schloss[1,†]

† To whom correspondence should be addressed: pschloss@umich.edu

1. Department of Microbiology and Immunology, University of Michigan, Ann Arbor, MI

2. Division of Infectious Diseases, Department of Internal Medicine, University of Michigan Medical School, Ann Arbor, MI 3. Unit for Laboratory Animal Medicine, University of Michigan, Ann Arbor, MI

Abstract

Clostridioides difficile infection (CDI) disease severity has increased over the last few decades. Patient age, white blood cell count, creatinine levels as well as *C. difficile* ribotype and toxin genes have been associated with disease severity. However, current models of CDI disease severity that incorporate these factors are not robust enough to be broadly applied. These models lack data describing the gut microbiota. Perturbations to the gut microbiota are necessary for *C. difficile* to colonize the gut. The gut microbiota is thought to impair *C. difficile* colonization through bile acid metabolism, nutrient consumption and bacteriocin production. It has been unclear whether the gut microbiota affect CDI disease severity. However, here we demonstrate that gut bacterial communities can contribute to disease severity. We derived diverse gut communities by colonizing germ-free mice with different human fecal communities. The mice were then infected with a single *C. difficile* RT027 clinical isolate which resulted in moribundity and histopathologic differences. The variation in severity was associated with the human fecal community that the mice received. Generally, facultative anaerobes with pathogenic potential, such as *Escherichia*, *Helicobacter*, and *Klebsiella*, were associated with more severe outcomes. Bacterial groups associated with fiber degradation, such as *Coprobacillus*, were associated with less severe outcomes. Finally, we showed that, when infected with a different *C. difficile* isolate, the outcome of the infection was similar between the mice that received the same fecal donor community. These data have demonstrated that the gut bacteria can influence CDI disease severity and may improve clinical models.

Importance

Clostridioides difficile infections (CDI) can be asymptomatic or range in severity from mild diarrhea to severe outcomes including surgical interventions and death. Models that predict severity and guide treatment decisions are based on clinical factors and *C. difficile*

characteristics. Although the gut microbiome plays a role in protecting against CDI, it has not been investigated for its effect on CDI disease severity or incorporated into attempts to predict disease severity. We demonstrated that variation in the microbiome of mice colonized with human feces was sufficient to result in a range of disease outcomes. These results revealed groups of bacteria associated with both severe and mild *C. difficile* infection outcomes. Gut bacterial community data from patients with CDI could improve our ability to identify patients at risk of developing more severe disease and improve interventions which treat the gut bacteria to reduce host damage.

Introduction

Clostridioides difficile infections (CDI) have increased in incidence and severity since *C. difficile* was first identified as the cause of antibiotic-associated pseudomembranous colitis (1). CDI disease severity can range from asymptomatic to mild diarrhea to toxic megacolon and death. Treatment for CDI is driven by the disease severity. The Infectious Diseases Society of America (IDSA) and Society for Healthcare Epidemiology of America (SHEA) guidelines categorize severe disease based on white blood cell count greater than 15,000 cells/mm^3 and/or a serum creatinine greater than 1.5 mg/dL, and complicated disease based on systolic blood pressure below 90, ileus, or toxic megacolon (2). Since these measures are only present once the disease has advanced, the IDSA classification does not allow for identification of patients at risk of severe CDI. Thus, we have limited ability to prevent patients from developing severe CDI. Ideally, we could identify patients that are high-risk of severe disease and adjust their treatments to halt the disease before it worsens.

Prediction models have been developed to score a patients risk for severe CDI outcomes but have not been robust for broad application (3–6). There is no widely accepted definition of severe disease (7). While the IDSA guideline is frequently used, many studies develop their own severity definitions. Aside from the features utilized by the IDSA guidelines, other severity measures use patient demographics, vital information, laboratory test results, disease complications, or infection outcomes such as ICU admission, surgery and/or death (3, 8–10). However, a recent multi-center external validation of these scoring systems using a consistent severity definition - transfer or admission to the intensive care unit, colectomy, and/or death within 30 days of diagnosis - demonstrated a decline in performance and high false positivity rate (5). Thus, patient and clinical factors have not been sufficient to accurately identify patients at risk of severe CDI and may benefit from additional information involved in the development of CDI disease.

Severity has been associated with characteristics of *C. difficile* ribotypes, such as 027, and host factors (11). Ribotypes with genes for toxin TcdA/TcdB have the potential to disrupt the tight junctions between the intestinal epithelial cells (12). The presence of binary toxin CDT or mutations in *tcdC*, the negative regulator of toxin transcription, have been associated with increased virulence of TcdA/TcdB (12). In addition to the pathogenic potential of *C. difficile*, the response by the host also affects the disease severity. IgG antibody activity towards the TcdA/TcdB are decreased in both patients with symptomatic and recurrent infections (13). In addition to controlling the infection, the immune response can also cause intestinal injury. Increased neutrophil inflitration into the mucosa after the cellular tight junctions have been compromised can exacerbate the inflammatory response (14). While we have have elucidated these major drivers of host damage in CDI, these are also the drivers of features of the poorly performing prediction models.

Missing from CDI severity prediction models are the effects of the indigenous gut bacteria. *C. difficile* interacts with the gut community in many ways. The indigenous bacteria of a healthy intestinal community provide a protective barrier preventing *C. difficile* from infecting the gut. A range of mechanisms can disrupt this barrier, including antibiotics, medications, or dietary changes, and lead to increased susceptiblity to CDI (15–17). Once in the gut, the indigenous bacteria can either promote or inhibit *C. difficile* through producing molecules or modifying the environment (18). Bile acids metabolized by the gut bacteria can inhibit *C. difficile* growth and affect toxin production (19, 20). Bacteria in the gut also can compete more directly with *C. difficile* through antibiotic production or nutrient consumption (21, 22). While the relationship between the gut bacteria and *C. difficile* has been established, the effect the gut bacteria can have on CDI disease severity is unclear. Recent studies have begun to uncover this relationship but have either used clinical data, which does not permit control of the host or *C. difficile* variation (23) or murine experiments, which lack variation in the bacterial communities (3). Recently, Tomkovich et al. showed the variation in the bacterial communities between mice from different mouse colonies resulted in different

clearance rates of *C. difficile* (24). Therefore, it is clear the gut bacteria modulate the activity and infection dynmaics of *C. difficile*. We hypothesized that gut bacteria also contribute to the variation in CDI disease severity. Here, we colonized germ-free C57BL/6 mice with human fecal communities to test whether the variability in the gut bacteria can produce and explain variation in disease severity.

Results

***C. difficile* is able to infect germ-free mice colonized with human fecal microbial communities without perturbation.** To produce gut microbiomes with greater variation than those found in conventional mouse colonies, we colonized germ-free mice with bacteria from human feces (25). We inoculated germ-free C57BL/6 mice with homogenized feces from one of 15 human fecal samples via oral gavage. The human fecal samples were selected because they represented diverse community structures based on community clustering (26). The gut communities were allowed to establish themselves for two weeks post inoculation (27). We then surveyed the bacterial members of the gut communities by 16S rRNA gene sequencing of fecal pellets (Figure 1A). The bacterial communities from each mouse grouped more closely to those communities from mice that received the same human fecal donor community than to the mice who received a different human fecal donor community (Figure 1B). The communities were primarily composed of populations of *Clostridia*, *Bacteroidia*, *Erysipelotrichia*, *Bacilli*, and *Gammaproteobacteria*. However, each group of mice harbored unique combination of class relative abundances in their gut bacterial communities.

Next, we tested this set of mice with their human-derived gut microbial communities for susceptibility to *C. difficile* infection. A typical mouse model of CDI requires pre-treatment with antibiotics, such as clindamycin, to become susceptible to *C. difficile* colonization (28, 29). However, we wanted to avoid modifying the communities with an antibiotic to maintain

their unique microbial compositions and ecological relationships. Since these communities came from people who have increased risk of CDI, such as hospitalization or recent antibiotic use (26), we decided to test if *C. difficile* was able to infect these mice without any antibiotic perturbation. We hypothesized that *C. difficile* would be able to colonize a subset of mice whose communities were susceptible from perturbations either the donor experienced or from the ecological selection when colonizing the murine gut. Mice were challenged with 10^3 *C. difficile* ribotype 027 human isolate 431 spores. The mice were followed for 10 days post-challenge and their stool was collected and plated for *C. difficile* colony forming units (CFU) to determine the extent of the infection. Suprisingly, mice from all donors were colonized (Figure 2). Only two mice were able to resist *C. difficile* infection and both received their community from the same donor, N3. By colonizing germ-free mice with different human fecal communities, we were able to generate diverse gut communities in mice, which were susceptible to *C. difficile* infection without further modification of the gut community.

Infection severity varies by initial community. After we challenged the mice with *C. difficile*, we investigated the outcome from the infection and its relationship to the initial community. We followed the mice for 10 days post-challenge for colonization density, toxin production, and mortality. Seven mice, from Donors N1, N2 and N5, were not colonized on the day after *C. difficile* challenge but were infected (>10^6) by the end of the experiment. All mice that received their community from Donor M1 through M6 succumbed to the infection and became moribund within 3 days post-challenge. The remaining mice, except the uninfected Donor N3 mice, maintained *C. difficile* infection through the end of the experiment (Figure 2). At 10 days post-challenge, or earlier for the moribund mice, mice were euthanised and fecal pellets were assayed for toxin activity and cecal tissue was collected and scored for histopathologic signs of disease (Figure 3). Overall, there was greater toxin activity detected in the stool of the moribund mice (P = 0.003). However, when looking at each group of mice, we saw there was a range in toxin activity for both the

moribund and non-moribund mice (Figure 3A). Non-moribund mice from Donors N4 through N9 had comparable toxin activity as the moribund mice. Additionally, not all moribund mice had toxin activity detected in their stool. This discordance between toxin activity and disease severity has been previously described (30, 31). Next we examined the cecal tissue for histopathologic damage. Moribund mice had high levels of epithelial damage, tissue edema and inflammation (Figure S1), similar to previously reported histopathologic findings for *C. difficile* ribotype 027 (32). As observed with toxin activity, the moribund mice had higher histopathologic scores than the non-moribund mice (P = 3.0e-9). However, unlike the toxin activity, all moribund mice had consistently high histopathologic summary scores (Figure 3B). The non-moribund mice, Donor groups N1 through N9, had a range in tissue damage from none detected to similar levels as the moribund mice, which grouped by community donor. Together, the toxin activity, histopathologic score, and moribundity showed variation across the donor groups but were largely consistent within each donor group.

Microbial community members explain variation in CDI severity. We next interrogated the bacterial communities at the time of *C. difficile* challenge (day 0) for their relationship to infection outcomes using linear discriminant analysis (LDA) effect size (LEfSe) analysis to identify individual bacterial populations that could explain the variation in disease severity. We split the mice into groups by severity level based on their moribundity and histopathologic score. We dichotomized the histopathologic scores into high and low groups by splitting on the median score. This analysis revealed 20 genera that were significantly different by the disease severity (Figure 4A). Bacterial genera *Turicibacter*, *Streptococcus*, *Staphylococcus*, *Pseudomonas*, *Phocaeicola*, *Parabacteroides*, *Bacteroides*, and *Escherichia/Shigella* were detected at higher relative abundances in the mice that became moribund. Populations of *Anaerotignum*, *Coprobacillus*, *Enterocloster*, and *Murimonas* were more abundant in the non-moribund mice that would develop only low intestinal injury. To understand the role of toxin

activity in disease severity, we applied LEfSe to identify the genera most likely to explain the observed differences in toxin activity (Figure 4B). Many genera that associated with toxin production were also associated with moribundity, such as populations of *Escherichia/Shigella* and *Bacteroides*. Likewise, there were genera such as *Anaerotignum*, *Enterocloster*, and *Murimonas* that associated with no toxin that also exhibited greater relative abundance in communities from non-moribund mice with a low histopathologic score. Lastly, we tested for correlations between the endpoint relative abundances of bacterial operational taxonomic units (OTUs) and the histopathologic summary score (Figure 4C). The endpoint relative abundance of *Bacteroides* was positively correlated with histopathologic score, as its day 0 relative abundance did with disease severity (Figure 4A). Populations of *Klebsiella* and *Prevotellaceae* were positively correlated with the histopathologic score and were increased in the group of mice with detectable toxin. This analysis has revealed bacterial genera that associated with the variation in moribundity, histopathologic score, and toxin activity of CDI.

We next determined whether collectively, bacterial community membership and relative abundance could be predictive of the CDI disease outcome. We trained random forest models with bacterial community relative abundance data from the day of colonization at each taxonomic rank to predict toxin production, moribundity, and day 10 post-challenge histopathologic summary score. For predicting if toxin would be produced, microbial populations aggregated by phylum rank classification performed similarly as models using lower taxonomic ranks (AUROC = 0.83, Figure S2). *C. difficile* was more likely to produce toxin when the community it infected had less abundant populations of *Verrucomicrobia* and *Campilobacterota* and had more abundant populations of *Proteobacteria* (Figure 5A). Next, we assessed the ability of the community to predict moribundity. Bacteria grouped by class rank classification was sufficient to predict which mice would succumb to the infection before the end of the experiment (AUROC = 0.91, Figure S2). THe features with the greatest effect showed that communities with greater populations of bacteria belonging to

Bacilli and *Firmicutes* and reduced populations of *Erysipelotrichia* were more likely to result in moribundity (Figure 5B). Only one other class of bacteria was decreased in moribund mice, a group of unclassified *Clostridia*. Lastly, the relative abundances of genera were able to predict a high or low histopathologic score (histopathologic scores were dichotomized as in previous analysis, AUROC = 0.99, Figure S2). No genera had a significantly greater effect on the model performance than any others, indicating the model is reliant on many genera for the correct prediction. The model used some of the genera identified in the LEfSe analysis, such as *Coprobacillus*, *Anaerostipes*, and *Hungatella*. Communities with greater abundances of *Hungatella*, *Eggerthella*, *Bifidobacterium*, *Duncaniella* and *Neisseria* were more likely to have high histopathologic scores. These models have shown that the relative abundance of bacterial populations and their relationship to each other could be used to predict the variation in moribundity, histopathologic score, and toxin activity of CDI.

Disease severity consistent by donor community across isolates. Since Carlson et al. showed clinical disease severity varied by *C. difficile* isolate characteristics, such as germination rate (33, 34), we next tested whether the effect of the community on CDI outcomes was conserved across *C. difficile* isolates. We colonized mice with human fecal slurry of either Donor N7, N6, or M4 and allowed two weeks for the community to establish. We then challenged the mice with a different *C. difficile* isolate and all mice were infected. The moribundity and histopathologic score outcomes when challenged with a different *C. difficile* human isolate were comparable to the outcomes of challenges with *C. difficile* ribotype 027 human isolate 431 by their donor group (Figure 6). For the isolates and communities we tested, the effect of the gut bacterial community on disease severity was greater than the effect of the variation in these isolates.

Discussion

Challenging mice colonized with different human fecal communities with a single *C. difficile* isolate, ribotype 027 isolate 431, demonstrated the variation in the gut bacteria affects the *C. difficile* infection disease severity. Our analysis revealed an association between the relative abundance of bacterial community members and disease severity. We used the relative abundance patterns of community members associated with disease outcomes to select donor communities to test whether the disease severity was conserved when challenged with a different *C. difficile* isolate. The disease outcomes from the challenge with the second *C. difficile* isolate matched the outcomes of the challenge with *C. difficile* ribotype 027 isolate 431. Therefore, the effect of the community variation on disease severity *in vivo* was greater than the effect of *C. difficile* isolate variation (33, 34). Overall, these results have demonstrated that the bacterial community contributed to the disease severity of *C. difficile* infection.

CDI severity can range from no symptoms to mild symptoms, such as diarrhea, to severe symptoms, such as toxic megacolon or death. Physicians use prediction tools to identify patients most at risk of developing a severe infection using white blood cell counts, serum albumin level, or serum creatinine level (2, 8, 35). Those levels are driven by the activities in the intestine (36). Research into the drivers of this variation have revealed factors that make *C. difficile* more virulent. Strains are categorized for their virulence by the presence and production toxin TcdA, toxin TcdB, and binary toxin and the prevelance in outbreaks, such as ribotypes 027 and 078 (28, 37–40). However, other studies have shown that virulence is not necessarily linked with toxin production (41) or the strain (42). Furthermore, there is variation in the genome, growth rate, sporulation, germination, and toxin production in different isolates of a strain (33, 34, 43). This variation may help explain why severe CDI prediction tools often miss identifying many patients with CDI that will develop severe disease (3–6). Therefore, it is necessary to gain a full understanding of all

factors contributing to disease variation to improve our ability to predict severity.

The state of the gut bacterial community determines the ability of *C. difficile* to colonize, persist in the intestine. *C. difficile* is unable to colonize an unperturbed healthy gut community and is only able to become established after a perturbation (29). Once colonized, the different communities lead to different metabolic responses and dynamics of the *C. difficile* population (44–46). The gut bacteria metabolize primary bile acids into secondary bile acids (47, 48). The concentration of these bile acids affect the germination, growth, toxin production and biofilm formation (19, 20, 49, 50). Members of the bacterial community also affect other metabolites *C. difficile* utilizes. *Bacteroides thetaiotaomicron* produce sialidases which release sialic acid from the mucosa for *C. difficile* to utilize (51, 52). The nutrient environment affects toxin production (53). Thus, many of the actions of the gut bacteria modulate *C. difficile* in ways that could affect the infection and resultant disease.

Myriad studies have explored the relationship between the microbiome and CDI but none have established a relationship between the variation of disease severity and the microbiome. CDI studies often use an infection model with a single homogeneous bacterial community. Collins et al. used multiple human communities to colonize mice, however the communities were pooled prior to gavaging into germ-free mice (54), resulting in a single community. Studies examining difference in disease often use different *C. difficile* strains or ribotypes in mice with similar microbiota as a proxy for variation in disease, such as strain 630 for non-severe and ribotype 027 for severe (28, 37, 38, 55). Studies have also demonstrated variation in infection through tapering antibiotic dosage (29, 46, 56) or by reducing the amount of *C. difficile* cells or spores used for the challenge (28, 56). These studies either lack variation in the microbiome or have variation in the *C. difficile* infection itself, therefore we cannot make any association between variation in severity and the microbiome.

With our recent observations that the initial community affected the ability of *C. difficile* to persist in the gut (24, 46) and the existing research describing the myriad interactions between the microbiome and *C. difficile*, we hypothesized that the microbiome can modulate CDI disease severity. Our data have demonstrated gut bacterial relative abundances associate with variation in toxin production, histopathologic scoring of the cecal tissue and mortality. This analysis revealed populations of *Akkermansia*, *Anaerostipes*, *Coprobacillus*, *Enterocloster*, *Lactonifactor*, and *Monoglobus* were more abundant in the microbiome of non-moribund mice which had low histopathologic scores and no detected toxin. The protective role of these genera are supported by previous studies. *Coprobacillus*, *Lactonifactor*, and *Monoglobus* have been shown to be involved in dietary fiber fermentation and associated with healthy communities (57–60). *Anaerostipes* and *Coprobacillus*, which produce short chain fatty acids, have been associated with healthy communities (61–63). Furthermore, *Coprobacillus*, which was abundant in mice with low histopathologic scores but rare in all other mice, has been shown to contain a putative type I lantibiotic gene cluster and inhibit *C. difficile* colonization (64–66). *Akkermansia* and *Enterocloster* were also identified as more abundant in mice which had a low histopathologic scores but have contradictory supporting evidence in the current literature. In our data, *Akkermansia* was most abundant in the non-moribund mice with low histopathologic scores but there were some moribund mice which had increased populations of *Akkermansia*. This could be attributed to either a more protective mucus layer was present inhibiting colonization (66, 67) or mucus consumption by *Akkermansia* could have been crossfeeding *C. difficile* or exposing a niche for *C. difficile* (68–70). Similarly with *Enterocloster*, in our data this genus was more abundant and associated with low histopathologic scores. It has been associated with healthy populations and has been used to mono-colonize germ-free mice to reduce the ability of *C. difficile* to colonize (71, 72). However, *Enterocloster*, a member of indigenous gut communities, has been involved in infections, such as bacteremia (73, 74). These data have exemplified

populations of bacteria that have the potential to be either protective or harmful. Thus, the disease outcome is not likely based on the abundance of individual populations of bacteria, rather it is the result of the interactions of the community.

The groups of bacteria that were associated with either a higher histopathologic score or moribundity are members of the indigenous gut community that also have been associated with disease, often referred to as opportunistic pathogens. Many of the populations with pathogenic potential that associated with worse outcomes are also facultative anaerobes. *Enterococcus*, *Klebsiella*, *Shigella/Escherichia*, *Staphylococcus*, and *Streptococcus* have been shown to expand after antibiotic use (26, 75, 76) and are commonly detected in CDI cases (77–80). In addition to these populations, *Eggerthella*, *Prevotellaceae* and *Helicobacter*, which associated with worse outcomes, have also been associated with intestinal inflammation (81–83). Recently, *Helicobacter hepaticus* was shown to be sufficient to cause susceptibility to CDI in IL-10 deficient C57BL/6 mice (84). In our experiments, when *Helicobacter* was present, the infection resulted in a high histopathologic score. While we did not use IL-10 deficient mice, it is possible the bacterial community or host response are similarly modified by *Helicobacter*, allowing *C. difficile* infection and host damage. Aside from *Helicobacter*, these groups of bacteria that associated with more severe outcomes did not have a conserved association between their relative abundance and the disease severity across all mice.

Since we observed groups of bacteria that were associated with less severe disease in some case and either no effect or more severe disease in others, it may be more appropriate to apply the damage-response framework for microbial pathogenesis to CDI (85, 86). Disease is not driven by a single entity, rather it is an emergent property of the responses of the host immune system, infecting microbe, *C. difficile*, and the indigenous microbes at the site of infection. In the first set of experiments, we used the same host, C57BL/6 mice, the same infecting microbe, *C. difficile* ribotype 027 human isolate 431,

with different gut bacterial communities. The bacterial groups in those communities were often present in both moribund and non-moribund and across the range of histopathologic scores. Thus, it was not merely the presence of the bacteria but their activity in response to the other microbes and host which affect the extent of the host damage. Additionally, while each mouse and *C. difficile* population had the same genetic background, they too were reacting to the specific microbial community. Disease severity is driven by the cumulative effect of the host immune response and the activity of *C. difficile* and the gut bacteria. *C. difficile* can drive host damage through the production of toxin. The gut microbiota can contribute to the host damage through the balance of metabolic and competitive activities, such as bacteriocin production or mucin degradation. For example, low levels of mucin degradation can provide nutrients to other community members producing a diverse non-damaging community (87). However, if mucin degradation becomes too great it reduces the protective function of the mucin layer and exposes the epithelial cells. This over-harvesting can contribute to the host damage due to other members producing toxin. Thus, the resultant intestinal damage is the balance of all activities in the gut environment. Host damage is the emergent property of numerous damage-response curves, such as one for host immune response, one for *C. difficile* activity and another for microbiome community activity, each of which are a composite curve of the individual activities from each group, such as antibody production, neutrophil infiltration, toxin production, sporulation, fiber and mucin degradation. Therefore, while we have identified populations of interest, it may be necessary to target multiple types of bacteria to reduce the community interactions contributing to host damage.

Many studies have investigated individual activities that contribute to CDI. Here we have shown myriad bacterial groups and their relative abundances associated with variation in severity of CDI disease. We must continue to explore how host, microbiota, and *C. difficile* interactions result in severe outcomes. We may be able to reduce the risk of severity with a better understanding of which interactions, whether driven by specific community

functions or groups of bacteria, reduce host damage. Approaching this problem from a damage-response framework would expand the treatment to modifying multiple groups of bacteria and activities to reduce overall host damage. Our current clinical treatment for primary CDI targets an individual group of this tripartite system. Most commonly, CDI is treated with an antibiotic to eliminate *C. difficile*. Alternatively, another treatment uses antibodies to neutralize *C. difficile* toxins. These treatments are only addressing a single entity of the system, leaving the potential for the others to maintain responses that contribute to host damage. However, we may be able to improve CDI treatment through elucidating interventions that drive all three entities towards reduced host damage. When a patient is diagnosed with CDI, the gut community composition, in addition to the traditionally obtained clinical information, may improve our severity prediction and guide profilactic treatment. Treating the microbiome at the time of diagnosis may prevent the infection from becoming more severe. Based on the general trends of our results, promoting fiber metabolizing bacteria and reducing facultative anaerobes may bolster the efficacy of current CDI treatments, reducing disease severity.

Materials and Methods

Animal care. 6- to 13-week old male and female germ-free C57BL/6 were obtained from a single breeding colony in the University of Michigan Germ-free Mouse Core. Mice were housed in cages of 2-4 mice per cage and maintained in germ-free isolators at the University of Michigan germ-free facility. All mouse experiments were approved by the University Committee on Use and Care of Animals at the University of Michigan. **Were the mice maintained in gnotobiotic isolators throughout the experiment? Or were they transferred to BSL2 conditions prior to administering the human FMTs?**

***C. difficile* experiments.** Human fecal samples were obtained from Schubert et al. and selected based on community clusters (26) to result in diverse community structures. Feces

were homogenized by mixing 200 mg of sample with 5 ml of PBS. Mice were inoculated with 100 μl of the fecal homogenate via oral gavage. For the set of experiments testing multiple *C. difficile* clinical isolates, we selected a subset of donor fecal samples based on their associated mouse transplant communities and the outcomes in the experiments with *C. difficile* ribotype 027 isolate 431 that fit the following criteria: one community we would expect to result in a low histopathologic score (< 5), a high histopathologic score (> 5), and a high histopathologic score which becomes moribund. Additionally, we selected the donors based their relative abundances of genera identified through the our analysis (Figure S3). Two weeks after the fecal community inoculation, mice were challenged with *C. difficile*. *C. difficile* isolates came from Carlson et al. which had previously been isolated and characterized (33, 34). Spores concentration were determined both before and after challenge (88). 10^3 *C. difficile* spores were given to each mouse via oral gavage. **How were human FMTs prepared (anaerobically vs aerobically, etc)?**

Sample collection. Fecal samples were collected on the day of *C. difficile* challenge and the following 10 days. Each day, a fecal sample was also collected and weighed and the remaining sample was frozen at -20°C. Anaerobically, the weighed fecal samples were serially diluted in PBS, plated on TCCFA plates, and incubated at 37°C for 24 hours. The plates were then counted for the number of colony forming units (CFU) (89).

DNA sequencing. From the frozen fecal samples, total bacterial DNA was extracted using MOBIO PowerSoil-htp 96-well soil DNA isolation kit. We amplified the 16S rRNA gene V4 region and sequenced the resulting amplicons using an Illumina MiSeq as described previously (90).

Sequence curation. Sequences were processed with mothur(v.1.44.3) as previously described (90, 91). In short, we used a 3% dissimilarity cutoff to group sequences into operational taxonomic units (OTUs). We used a naive Bayesian classifier with the Ribosomal Database Project training set (version 18) to assign taxonomic classifications

to each OTU (92). We sequenced a mock community of a known community composition and 16s rRNA gene sequences. We processed this mock community with our samples to calculate the error rate for our sequence curation, which was an error rate of 0.19%.

Toxin cytotoxicity assay. Fecal sample remaining after plating for CFU and DNA extraction were collected in a preweighted sterile tube and stored at -80℃. To prepare the sample for the activity assay, samples were diluted 1:10 weight per volume using sterile PBS and then filter sterilized through a 0.22-μm filter. Toxin activity was assessed using a Vero cell rounding-based cytotoxicity assay as described previously (38). The cytotoxicity titer was determined for each sample as the last dilution, which resulted in at least 80% cell rounding. Toxin titers are reported as the log10 of the reciprocal of the cytotoxicity titer.

Histopathology evaluation. Mouse ceca tissue was placed in histopathology cassettes and fixed in 10% formalin, then stored in 70% ethanol. McClinchey Histology Labs, Inc. (Stockbridge, MI) embedded the samples in paraffin, sectioned, and created the hematoxylin and eosin-stained slides. The slides were scored using previously described criteria by a board-certified veterinary pathologist scored who was blinded to the experimental groups (38).

Statistical analysis and modeling. To compare community structures, we calculated Yue and Clayton dissimilarity matrices in mothur (93). We rarified samples to 2,107 sequences per sample to limit uneven sampling biases. We tested for differences in individual taxonomic groups that would explain the outcome differences with LEfSe (94) in mothur. Remaining statistical analysis and data visualization was performed in R (v4.0.5) with the tidyverse package (v1.3.1). We tested for significant differences in β-diversity (θ_{YC})using the Wilcoxon rank sum test. We used Spearman's corrlation to identified the OTU which had a correlation between their relative abundance and the histopathologic summary score. *P* values were then corrected for multiple comparisons with a Benjamini and Hochberg adjustment for a type I error rate of 0.05 (95). We built random forest models

using the mikropml package (96) with OTUs from day 0 samples using mtry values of 1 through 10, 15, 20, 25, 40, 50, 100. The split for training and testing varied by model to avoid overfitting the data. The toxin and moribundity models were trained with 60% of the data. The histopathologic score model was trained with 80% of the data. Lastly, we did not analyze murine communities to donor community or clinical data because germ-free mice colonized with human fecal communities become more like indigenous murine communities once stabilized. Futhermore, we are not trying to make any claims about human bacteria and their association with human CDI.

Code availability. Scripts necessary to reproduce our analysis and this paper are available in an online repository (https://github.com/SchlossLab/Lesniak_Severity_XXXX_2022).

Sequence data accession number. All 16S rRNA gene sequence data and associated metadata are available through the Sequence Read Archive via accession XXXX.

Acknowledgements

Thank you to Sarah Lucas and Sarah Tomkovich for critical discussion in the development and execution of this project. We also thank the University of Michigan Germ-free Mouse Core for assistance with our germfree mice, funded in part by U2CDK110768. This work was supported by several grants from the National Institutes for Health R01GM099514, U19AI090871, U01AI12455, and P30DK034933. Additionally, NAL was supported by the Molecular Mechanisms of Microbial Pathogenesis training grant (NIH T32 AI007528). The funding agencies had no role in study design, data collection and analysis, decision to publish, or preparation of the manuscript.

References

1. **Kelly CP**, **LaMont JT**. 2008. *Clostridium difficile* more difficult than ever **359**:1932–1940. doi:10.1056/nejmra0707500.

2. **McDonald LC**, **Gerding DN**, **Johnson S**, **Bakken JS**, **Carroll KC**, **Coffin SE**, **Dubberke ER**, **Garey KW**, **Gould CV**, **Kelly C**, **Loo V**, **Sammons JS**, **Sandora TJ**, **Wilcox MH**. 2018. Clinical practice guidelines for *Clostridium difficile* infection in adults and children: 2017 update by the infectious diseases society of america (IDSA) and society for healthcare epidemiology of america (SHEA). Clinical Infectious Diseases **66**:e1–e48. doi:10.1093/cid/cix1085.

3. **Dieterle MG**, **Putler R**, **Perry DA**, **Menon A**, **Abernathy-Close L**, **Perlman NS**, **Penkevich A**, **Standke A**, **Keidan M**, **Vendrov KC**, **Bergin IL**, **Young VB**, **Rao K**. 2020. Systemic inflammatory mediators are effective biomarkers for predicting adverse outcomes in *Clostridioides difficile* infection. mBio **11**. doi:10.1128/mbio.00180-20.

4. **Butt E**, **Foster JA**, **Keedwell E**, **Bell JE**, **Titball RW**, **Bhangu A**, **Michell SL**, **Sheridan R**. 2013. Derivation and validation of a simple, accurate and robust prediction rule for risk of mortality in patients with *Clostridium difficile* infection. BMC Infectious Diseases **13**. doi:10.1186/1471-2334-13-316.

5. **Perry DA**, **Shirley D**, **Micic D**, **Patel CP**, **Putler R**, **Menon A**, **Young VB**, **Rao K**. 2021. External validation and comparison of *Clostridioides difficile* severity scoring systems. Clinical Infectious Diseases. doi:10.1093/cid/ciab737.

6. **Beurden YH van**, **Hensgens MPM**, **Dekkers OM**, **Cessie SL**, **Mulder CJJ**, **Vandenbroucke-Grauls CMJE**. 2017. External validation of three prediction tools for patients at risk of a complicated course of *Clostridium difficile* infection: Disappointing in an outbreak setting. Infection Control & Hospital Epidemiology **38**:897–905.

doi:10.1017/ice.2017.89.

7. **Ressler A**, **Wang J**, **Rao K**. 2021. Defining the black box: A narrative review of factors associated with adverse outcomes from severe clostridioides difficile infection **14**:175628482110481. doi:10.1177/17562848211048127.

8. **Zar FA**, **Bakkanagari SR**, **Moorthi KMLST**, **Davis MB**. 2007. A comparison of vancomycin and metronidazole for the treatment of *Clostridium difficile*-associated diarrhea, stratified by disease severity. Clinical Infectious Diseases **45**:302–307. doi:10.1086/519265.

9. **Gujja D**, **Friedenberg FK**. 2009. Predictors of serious complications due toClostridium difficileinfection **29**:635–642. doi:10.1111/j.1365-2036.2008.03914.x.

10. **Jardin CGM**, **Palmer HR**, **Shah DN**, **Le F**, **Beyda ND**, **Jiang Z**, **Garey KW**. 2013. Assessment of treatment patterns and patient outcomes before vs after implementation of a severity-based *Clostridium difficile* infection treatment policy **85**:28–32. doi:10.1016/j.jhin.2013.04.017.

11. **Bauer MP**, **Notermans DW**, **Benthem BH van**, **Brazier JS**, **Wilcox MH**, **Rupnik M**, **Monnet DL**, **Dissel JT van**, **Kuijper EJ**. 2011. *Clostridium difficile* infection in europe: A hospital-based survey **377**:63–73. doi:10.1016/s0140-6736(10)61266-4.

12. **Abt MC**, **McKenney PT**, **Pamer EG**. 2016. *Clostridium difficile* colitis: Pathogenesis and host defence **14**:609–620. doi:10.1038/nrmicro.2016.108.

13. **Kelly CP**, **Kyne L**. 2011. The host immune response to *Clostridium difficile* **60**:1070–1079. doi:10.1099/jmm.0.030015-0.

14. **Farooq PD**, **Urrunaga NH**, **Tang DM**, **Rosenvinge EC von**. 2015. Pseudomembranous colitis **61**:181–206. doi:10.1016/j.disamonth.2015.01.006.

15. **Britton RA**, **Young VB**. 2014. Role of the intestinal microbiota in resistance to colonization by *Clostridium difficile* **146**:1547–1553. doi:10.1053/j.gastro.2014.01.059.

16. **Hryckowian AJ**, **Treuren WV**, **Smits SA**, **Davis NM**, **Gardner JO**, **Bouley DM**, **Sonnenburg JL**. 2018. Microbiota-accessible carbohydrates suppress *Clostridium difficile* infection in a murine model **3**:662–669. doi:10.1038/s41564-018-0150-6.

17. **Vila AV**, **Collij V**, **Sanna S**, **Sinha T**, **Imhann F**, **Bourgonje AR**, **Mujagic Z**, **Jonkers DMAE**, **Masclee AAM**, **Fu J**, **Kurilshikov A**, **Wijmenga C**, **Zhernakova A**, **Weersma RK**. 2020. Impact of commonly used drugs on the composition and metabolic function of the gut microbiota **11**. doi:10.1038/s41467-019-14177-z.

18. **Abbas A**, **Zackular JP**. 2020. Microbe-microbe interactions during *Clostridioides difficile* infection **53**:19–25. doi:10.1016/j.mib.2020.01.016.

19. **Sorg JA**, **Sonenshein AL**. 2008. Bile salts and glycine as cogerminants for *Clostridium difficile* spores. Journal of Bacteriology **190**:2505–2512. doi:10.1128/jb.01765-07.

20. **Thanissery R**, **Winston JA**, **Theriot CM**. 2017. Inhibition of spore germination, growth, and toxin activity of clinically relevant *C. difficile* strains by gut microbiota derived secondary bile acids. Anaerobe **45**:86–100. doi:10.1016/j.anaerobe.2017.03.004.

21. **Aguirre AM**, **Yalcinkaya N**, **Wu Q**, **Swennes A**, **Tessier ME**, **Roberts P**, **Miyajima F**, **Savidge T**, **Sorg JA**. 2021. Bile acid-independent protection against *Clostridioides difficile* infection **17**:e1010015. doi:10.1371/journal.ppat.1010015.

22. **Kang JD**, **Myers CJ**, **Harris SC**, **Kakiyama G**, **Lee I-K**, **Yun B-S**, **Matsuzaki K**, **Furukawa M**, **Min H-K**, **Bajaj JS**, **Zhou H**, **Hylemon PB**. 2019. Bile acid 7α-dehydroxylating gut bacteria secrete antibiotics that inhibit *Clostridium difficile*: Role of secondary bile acids **26**:27–34.e4. doi:10.1016/j.chembiol.2018.10.003.

527 23. **Seekatz AM**, **Rao K**, **Santhosh K**, **Young VB**. 2016. Dynamics of the fecal
528 microbiome in patients with recurrent and nonrecurrent *Clostridium difficile* infection **8**.
529 doi:10.1186/s13073-016-0298-8.

530 24. **Tomkovich S**, **Stough JMA**, **Bishop L**, **Schloss PD**. 2020. The initial gut microbiota
531 and response to antibiotic perturbation influence *Clostridioides difficile* clearance in mice.
532 mSphere **5**. doi:10.1128/msphere.00869-20.

533 25. **Nagpal R**, **Wang S**, **Woods LCS**, **Seshie O**, **Chung ST**, **Shively CA**, **Register**
534 **TC**, **Craft S**, **McClain DA**, **Yadav H**. 2018. Comparative microbiome signatures
535 and short-chain fatty acids in mouse, rat, non-human primate, and human feces **9**.
536 doi:10.3389/fmicb.2018.02897.

537 26. **Schubert AM**, **Rogers MAM**, **Ring C**, **Mogle J**, **Petrosino JP**, **Young VB**,
538 **Aronoff DM**, **Schloss PD**. 2014. Microbiome data distinguish patients with *Clostridium*
539 *difficile* infection and non-*C. difficile*-associated diarrhea from healthy controls **5**.
540 doi:10.1128/mbio.01021-14.

541 27. **Gillilland MG**, **Erb-Downward JR**, **Bassis CM**, **Shen MC**, **Toews GB**, **Young**
542 **VB**, **Huffnagle GB**. 2012. Ecological succession of bacterial communities during
543 conventionalization of germ-free mice **78**:2359–2366. doi:10.1128/aem.05239-11.

544 28. **Chen X**, **Katchar K**, **Goldsmith JD**, **Nanthakumar N**, **Cheknis A**, **Gerding DN**, **Kelly**
545 **CP**. 2008. A mouse model of *Clostridium difficile*-associated disease. Gastroenterology
546 **135**:1984–1992. doi:10.1053/j.gastro.2008.09.002.

547 29. **Schubert AM**, **Sinani H**, **Schloss PD**. 2015. Antibiotic-induced alterations of
548 the murine gut microbiota and subsequent effects on colonization resistance against
549 *Clostridium difficile*. mBio **6**. doi:10.1128/mbio.00974-15.

550 30. 2006. Correlation of disease severity with fecal toxin levels in patients with

Clostridium difficile-associated diarrhea and distribution of PCR ribotypes and toxin yields in vitro of corresponding isolates. Journal of Clinical Microbiology **44**:353–358. doi:10.1128/jcm.44.2.353-358.2006.

31. **Vitucci JC**, **Pulse M**, **Tabor-Simecka L**, **Simecka J**. 2020. Epidemic ribotypes of *clostridium* (now *clostridioides*) *difficile* are likely to be more virulent than non-epidemic ribotypes in animal models. BMC Microbiology **20**. doi:10.1186/s12866-020-1710-5.

32. **Cowardin CA**, **Buonomo EL**, **Saleh MM**, **Wilson MG**, **Burgess SL**, **Kuehne SA**, **Schwan C**, **Eichhoff AM**, **Koch-Nolte F**, **Lyras D**, **Aktories K**, **Minton NP**, **Petri WA**. 2016. The binary toxin CDT enhances *Clostridium difficile* virulence by suppressing protective colonic eosinophilia. Nature Microbiology **1**. doi:10.1038/nmicrobiol.2016.108.

33. **Carlson PE**, **Walk ST**, **Bourgis AET**, **Liu MW**, **Kopliku F**, **Lo E**, **Young VB**, **Aronoff DM**, **Hanna PC**. 2013. The relationship between phenotype, ribotype, and clinical disease in human *Clostridium difficile* isolates. Anaerobe **24**:109–116. doi:10.1016/j.anaerobe.2013.04.003.

34. **Carlson PE**, **Kaiser AM**, **McColm SA**, **Bauer JM**, **Young VB**, **Aronoff DM**, **Hanna PC**. 2015. Variation in germination of clostridium difficile clinical isolates correlates to disease severity. Anaerobe **33**:64–70. doi:10.1016/j.anaerobe.2015.02.003.

35. **Lungulescu OA**, **Cao W**, **Gatskevich E**, **Tlhabano L**, **Stratidis JG**. 2011. CSI: A severity index for *Clostridium difficile* infection at the time of admission. Journal of Hospital Infection **79**:151–154. doi:10.1016/j.jhin.2011.04.017.

36. **Masi A di**, **Leboffe L**, **Polticelli F**, **Tonon F**, **Zennaro C**, **Caterino M**, **Stano P**, **Fischer S**, **Hägele M**, **Müller M**, **Kleger A**, **Papatheodorou P**, **Nocca G**, **Arcovito A**, **Gori A**, **Ruoppolo M**, **Barth H**, **Petrosillo N**, **Ascenzi P**, **Bella SD**. 2018. Human serum albumin is an essential component of the host defense mechanism against *Clostridium difficile*

intoxication. The Journal of Infectious Diseases **218**:1424–1435. doi:10.1093/infdis/jiy338.

37. **Abernathy-Close L**, **Dieterle MG**, **Vendrov KC**, **Bergin IL**, **Rao K**, **Young VB**. 2020. Aging dampens the intestinal innate immune response during severe *Clostridioides difficile* infection and is associated with altered cytokine levels and granulocyte mobilization. Infection and Immunity **88**. doi:10.1128/iai.00960-19.

38. **Theriot CM**, **Koumpouras CC**, **Carlson PE**, **Bergin II**, **Aronoff DM**, **Young VB**. 2011. Cefoperazone-treated mice as an experimental platform to assess differential virulence of *Clostridium difficile* strains. Gut Microbes **2**:326–334. doi:10.4161/gmic.19142.

39. **Goorhuis A**, **Bakker D**, **Corver J**, **Debast SB**, **Harmanus C**, **Notermans DW**, **Bergwerff AA**, **Dekker FW**, **Kuijper EJ**. 2008. Emergence of *Clostridium difficile* infection due to a new hypervirulent strain, polymerase chain reaction ribotype 078. Clinical Infectious Diseases **47**:1162–1170. doi:10.1086/592257.

40. **O'Connor JR**, **Johnson S**, **Gerding DN**. 2009. *Clostridium difficile* infection caused by the epidemic BI/NAP1/027 strain. Gastroenterology **136**:1913–1924. doi:10.1053/j.gastro.2009.02.073.

41. **Rao K**, **Micic D**, **Natarajan M**, **Winters S**, **Kiel MJ**, **Walk ST**, **Santhosh K**, **Mogle JA**, **Galecki AT**, **LeBar W**, **Higgins PDR**, **Young VB**, **Aronoff DM**. 2015. *Clostridium difficile* ribotype 027: Relationship to age, detectability of toxins a or b in stool with rapid testing, severe infection, and mortality. Clinical Infectious Diseases **61**:233–241. doi:10.1093/cid/civ254.

42. **Walk ST**, **Micic D**, **Jain R**, **Lo ES**, **Trivedi I**, **Liu EW**, **Almassalha LM**, **Ewing SA**, **Ring C**, **Galecki AT**, **Rogers MAM**, **Washer L**, **Newton DW**, **Malani PN**, **Young VB**, **Aronoff DM**. 2012. *Clostridium difficile* ribotype does not predict severe infection. Clinical Infectious Diseases **55**:1661–1668. doi:10.1093/cid/cis786.

599 43. **He M**, **Sebaihia M**, **Lawley TD**, **Stabler RA**, **Dawson LF**, **Martin MJ**, **Holt KE**,
600 **Seth-Smith HMB**, **Quail MA**, **Rance R**, **Brooks K**, **Churcher C**, **Harris D**, **Bentley SD**,
601 **Burrows C**, **Clark L**, **Corton C**, **Murray V**, **Rose G**, **Thurston S**, **Tonder A van**, **Walker**
602 **D**, **Wren BW**, **Dougan G**, **Parkhill J**. 2010. Evolutionary dynamics of *Clostridium difficile*
603 over short and long time scales. Proceedings of the National Academy of Sciences
604 **107**:7527–7532. doi:10.1073/pnas.0914322107.

605 44. **Jenior ML**, **Leslie JL**, **Young VB**, **Schloss PD**. 2017. *Clostridium difficile* colonizes
606 alternative nutrient niches during infection across distinct murine gut microbiomes.
607 mSystems **2**. doi:10.1128/msystems.00063-17.

608 45. **Jenior ML**, **Leslie JL**, **Young VB**, **Schloss PD**. 2018. *Clostridium difficile* alters the
609 structure and metabolism of distinct cecal microbiomes during initial infection to promote
610 sustained colonization. mSphere **3**. doi:10.1128/msphere.00261-18.

611 46. **Lesniak NA**, **Schubert AM**, **Sinani H**, **Schloss PD**. 2021. Clearance of *Clostridioides*
612 *difficile* colonization is associated with antibiotic-specific bacterial changes. mSphere **6**.
613 doi:10.1128/msphere.01238-20.

614 47. **Staley C**, **Weingarden AR**, **Khoruts A**, **Sadowsky MJ**. 2016. Interaction of gut
615 microbiota with bile acid metabolism and its influence on disease states. Applied
616 Microbiology and Biotechnology **101**:47–64. doi:10.1007/s00253-016-8006-6.

617 48. **Long SL**, **Gahan CGM**, **Joyce SA**. 2017. Interactions between gut bacteria and bile in
618 health and disease. Molecular Aspects of Medicine **56**:54–65. doi:10.1016/j.mam.2017.06.002.

619 49. **Sorg JA**, **Sonenshein AL**. 2010. Inhibiting the initiation of *Clostridium difficile* spore
620 germination using analogs of chenodeoxycholic acid, a bile acid. Journal of Bacteriology
621 **192**:4983–4990. doi:10.1128/jb.00610-10.

622 50. **Dubois T**, **Tremblay YDN**, **Hamiot A**, **Martin-Verstraete I**, **Deschamps J**, **Monot M**,

Briandet R, **Dupuy B**. 2019. A microbiota-generated bile salt induces biofilm formation in *Clostridium difficile*. npj Biofilms and Microbiomes **5**. doi:10.1038/s41522-019-0087-4.

51. **Ng KM**, **Ferreyra JA**, **Higginbottom SK**, **Lynch JB**, **Kashyap PC**, **Gopinath S**, **Naidu N**, **Choudhury B**, **Weimer BC**, **Monack DM**, **Sonnenburg JL**. 2013. Microbiota-liberated host sugars facilitate post-antibiotic expansion of enteric pathogens. Nature **502**:96–99. doi:10.1038/nature12503.

52. **Ferreyra JA**, **Wu KJ**, **Hryckowian AJ**, **Bouley DM**, **Weimer BC**, **Sonnenburg JL**. 2014. Gut microbiota-produced succinate promotes *C. difficile* infection after antibiotic treatment or motility disturbance. Cell Host & Microbe **16**:770–777. doi:10.1016/j.chom.2014.11.003.

53. **Martin-Verstraete I**, **Peltier J**, **Dupuy B**. 2016. The regulatory networks that control *Clostridium difficile* toxin synthesis. Toxins **8**:153. doi:10.3390/toxins8050153.

54. **Collins J**, **Auchtung JM**, **Schaefer L**, **Eaton KA**, **Britton RA**. 2015. Humanized microbiota mice as a model of recurrent *Clostridium difficile* disease. Microbiome **3**. doi:10.1186/s40168-015-0097-2.

55. **Lawley TD**, **Clare S**, **Walker AW**, **Stares MD**, **Connor TR**, **Raisen C**, **Goulding D**, **Rad R**, **Schreiber F**, **Brandt C**, **Deakin LJ**, **Pickard DJ**, **Duncan SH**, **Flint HJ**, **Clark TG**, **Parkhill J**, **Dougan G**. 2012. Targeted restoration of the intestinal microbiota with a simple, defined bacteriotherapy resolves relapsing *Clostridium difficile* disease in mice. PLoS Pathogens **8**:e1002995. doi:10.1371/journal.ppat.1002995.

56. **Reeves AE**, **Theriot CM**, **Bergin IL**, **Huffnagle GB**, **Schloss PD**, **Young VB**. 2011. The interplay between microbiome dynamics and pathogen dynamics in a murine model of *Clostridium difficile* infection. Gut Microbes **2**:145–158. doi:10.4161/gmic.2.3.16333.

57. **Mabrok HB**, **Klopfleisch R**, **Ghanem KZ**, **Clavel T**, **Blaut M**, **Loh G**. 2011. Lignan

transformation by gut bacteria lowers tumor burden in a gnotobiotic rat model of breast cancer. Carcinogenesis **33**:203–208. doi:10.1093/carcin/bgr256.

58. **Kim CC**, **Healey GR**, **Kelly WJ**, **Patchett ML**, **Jordens Z**, **Tannock GW**, **Sims IM**, **Bell TJ**, **Hedderley D**, **Henrissat B**, **Rosendale DI**. 2019. Genomic insights from *Monoglobus pectinilyticus*: A pectin-degrading specialist bacterium in the human colon. The ISME Journal **13**:1437–1456. doi:10.1038/s41396-019-0363-6.

59. **Prado SBR do**, **Minguzzi BT**, **Hoffmann C**, **Fabi JP**. 2021. Modulation of human gut microbiota by dietary fibers from unripe and ripe papayas: Distinct polysaccharide degradation using a colonic in vitro fermentation model. Food Chemistry **348**:129071. doi:10.1016/j.foodchem.2021.129071.

60. **Muthuramalingam K**, **Singh V**, **Choi C**, **Choi SI**, **Kim YM**, **Unno T**, **Cho M**. 2019. Dietary intervention using (1, 3)/(1, 6)-β-glucan, a fungus-derived soluble prebiotic ameliorates high-fat diet-induced metabolic distress and alters beneficially the gut microbiota in mice model. European Journal of Nutrition **59**:2617–2629. doi:10.1007/s00394-019-02110-5.

61. **Han S-H**, **Yi J**, **Kim J-H**, **Lee S**, **Moon H-W**. 2019. Composition of gut microbiota in patients with toxigenic *clostridioides* (*clostridium*) *difficile*: Comparison between subgroups according to clinical criteria and toxin gene load. PLOS ONE **14**:e0212626. doi:10.1371/journal.pone.0212626.

62. **Duncan SH**, **Louis P**, **Flint HJ**. 2004. Lactate-utilizing bacteria, isolated from human feces, that produce butyrate as a major fermentation product. Applied and Environmental Microbiology **70**:5810–5817. doi:10.1128/aem.70.10.5810-5817.2004.

63. **Ye J**, **Lv L**, **Wu W**, **Li Y**, **Shi D**, **Fang D**, **Guo F**, **Jiang H**, **Yan R**, **Ye W**, **Li L**. 2018. Butyrate protects mice against methionineCholine-deficient diet-induced non-alcoholic

steatohepatitis by improving gut barrier function, attenuating inflammation and reducing endotoxin levels. Frontiers in Microbiology **9**. doi:10.3389/fmicb.2018.01967.

64. **Walsh CJ**, **Guinane CM**, **O'Toole PW**, **Cotter PD**. 2017. A profile hidden markov model to investigate the distribution and frequency of LanB-encoding lantibiotic modification genes in the human oral and gut microbiome. PeerJ **5**:e3254. doi:10.7717/peerj.3254.

65. **Sandiford SK**. 2018. Current developments in lantibiotic discovery for treating *Clostridium difficile* infection. Expert Opinion on Drug Discovery **14**:71–79. doi:10.1080/17460441.2019.1549032.

66. **Stein RR**, **Bucci V**, **Toussaint NC**, **Buffie CG**, **Rätsch G**, **Pamer EG**, **Sander C**, **Xavier JB**. 2013. Ecological modeling from time-series inference: Insight into dynamics and stability of intestinal microbiota. PLoS Computational Biology **9**:e1003388. doi:10.1371/journal.pcbi.1003388.

67. **Nakashima T**, **Fujii K**, **Seki T**, **Aoyama M**, **Azuma A**, **Kawasome H**. 2021. Novel gut microbiota modulator, which markedly increases *Akkermansia muciniphila* occupancy, ameliorates experimental colitis in rats. Digestive Diseases and Sciences. doi:10.1007/s10620-021-07131-x.

68. **Geerlings S**, **Kostopoulos I**, **Vos W de**, **Belzer C**. 2018. *Akkermansia muciniphila* in the human gastrointestinal tract: When, where, and how? Microorganisms **6**:75. doi:10.3390/microorganisms6030075.

69. **Deng H**, **Yang S**, **Zhang Y**, **Qian K**, **Zhang Z**, **Liu Y**, **Wang Y**, **Bai Y**, **Fan H**, **Zhao X**, **Zhi F**. 2018. *Bacteroides fragilis* prevents *Clostridium difficile* infection in a mouse model by restoring gut barrier and microbiome regulation. Frontiers in Microbiology **9**. doi:10.3389/fmicb.2018.02976.

70. **Engevik MA**, **Engevik AC**, **Engevik KA**, **Auchtung JM**, **Chang-Graham AL**,

Ruan W, **Luna RA**, **Hyser JM**, **Spinler JK**, **Versalovic J**. 2020. Mucin-degrading microbes release monosaccharides that chemoattract *Clostridioides difficile* and facilitate colonization of the human intestinal mucus layer. ACS Infectious Diseases **7**:1126–1142. doi:10.1021/acsinfecdis.0c00634.

71. **Reeves AE**, **Koenigsknecht MJ**, **Bergin IL**, **Young VB**. 2012. Suppression of *Clostridium difficile* in the gastrointestinal tracts of germfree mice inoculated with a murine isolate from the family *lachnospiraceae*. Infection and Immunity **80**:3786–3794. doi:10.1128/iai.00647-12.

72. **Ma L**, **Keng J**, **Cheng M**, **Pan H**, **Feng B**, **Hu Y**, **Feng T**, **Yang F**. 2021. Gut microbiome and serum metabolome alterations associated with isolated dystonia. mSphere **6**. doi:10.1128/msphere.00283-21.

73. **Haas KN**, **Blanchard JL**. 2020. Reclassification of the *Clostridium clostridioforme* and *Clostridium sphenoides* clades as *enterocloster* gen. Nov. And *lacrimispora* gen. Nov., including reclassification of 15 taxa. International Journal of Systematic and Evolutionary Microbiology **70**:23–34. doi:10.1099/ijsem.0.003698.

74. **Finegold SM**, **Song Y**, **Liu C**, **Hecht DW**, **Summanen P**, **Könönen E**, **Allen SD**. 2005. *Clostridium clostridioforme*: A mixture of three clinically important species. European Journal of Clinical Microbiology & Infectious Diseases **24**:319–324. doi:10.1007/s10096-005-1334-6.

75. **VanInsberghe D**, **Elsherbini JA**, **Varian B**, **Poutahidis T**, **Erdman S**, **Polz MF**. 2020. Diarrhoeal events can trigger long-term *Clostridium difficile* colonization with recurrent blooms **5**:642–650. doi:10.1038/s41564-020-0668-2.

76. **Garza-González E**, **Mendoza-Olazarán S**, **Morfin-Otero R**, **Ramírez-Fontes A**, **Rodríguez-Zulueta P**, **Flores-Treviño S**, **Bocanegra-Ibarias P**, **Maldonado-Garza H**,

719 **Camacho-Ortiz A**. 2019. Intestinal microbiome changes in fecal microbiota transplant
720 (FMT) vs. FMT enriched with *lactobacillus* in the treatment of recurrent *Clostridioides*
721 *difficile* infection **2019**:1–7. doi:10.1155/2019/4549298.

722 77. **Shafiq M**, **Alturkmani H**, **Zafar Y**, **Mittal V**, **Lodhi H**, **Ullah W**, **Brewer J**. 2020.
723 Effects of co-infection on the clinical outcomes of *Clostridium difficile* infection **12**.
724 doi:10.1186/s13099-020-00348-7.

725 78. **Keith JW**, **Dong Q**, **Sorbara MT**, **Becattini S**, **Sia JK**, **Gjonbalaj M**, **Seok R**,
726 **Leiner IM**, **Littmann ER**, **Pamer EG**. 2020. Impact of antibiotic-resistant bacteria
727 on immune activation and *Clostridioides difficile* infection in the mouse intestine **88**.
728 doi:10.1128/iai.00362-19.

729 79. **Zackular JP**, **Moore JL**, **Jordan AT**, **Juttukonda LJ**, **Noto MJ**, **Nicholson MR**, **Crews**
730 **JD**, **Semler MW**, **Zhang Y**, **Ware LB**, **Washington MK**, **Chazin WJ**, **Caprioli RM**, **Skaar**
731 **EP**. 2016. Dietary zinc alters the microbiota and decreases resistance to *Clostridium*
732 *difficile* infection **22**:1330–1334. doi:10.1038/nm.4174.

733 80. **Berkell M**, **Mysara M**, **Xavier BB**, **Werkhoven CH van**, **Monsieurs P**, **Lammens**
734 **C**, **Ducher A**, **Vehreschild MJGT**, **Goossens H**, **Gunzburg J de**, **Bonten MJM**,
735 **Malhotra-Kumar S**. 2021. Microbiota-based markers predictive of development of
736 *Clostridioides difficile* infection **12**. doi:10.1038/s41467-021-22302-0.

737 81. **Gardiner BJ**, **Tai AY**, **Kotsanas D**, **Francis MJ**, **Roberts SA**, **Ballard SA**,
738 **Junckerstorff RK**, **Korman TM**. 2014. Clinical and microbiological characteristics of
739 *Eggerthella lenta* bacteremia **53**:626–635. doi:10.1128/jcm.02926-14.

740 82. **Iljazovic A**, **Roy U**, **Gálvez EJC**, **Lesker TR**, **Zhao B**, **Gronow A**, **Amend L**, **Will**
741 **SE**, **Hofmann JD**, **Pils MC**, **Schmidt-Hohagen K**, **Neumann-Schaal M**, **Strowig T**. 2020.
742 Perturbation of the gut microbiome by *prevotella* spp. Enhances host susceptibility to

743 mucosal inflammation **14**:113–124. doi:10.1038/s41385-020-0296-4.

744 83. **Nagalingam NA**, **Robinson CJ**, **Bergin IL**, **Eaton KA**, **Huffnagle GB**, **Young VB**.
745 2013. The effects of intestinal microbial community structure on disease manifestation in
746 IL-$10^{-/-}$ mice infected with helicobacter hepaticus **1**. doi:10.1186/2049-2618-1-15.

747 84. **Abernathy-Close L**, **Barron MR**, **George JM**, **Dieterle MG**, **Vendrov KC**, **Bergin**
748 **IL**, **Young VB**. 2021. Intestinal inflammation and altered gut microbiota associated with
749 inflammatory bowel disease render mice susceptible to *Clostridioides difficile* colonization
750 and infection. doi:10.1128/mbio.02733-20.

751 85. **Pirofski L-a**, **Casadevall A**. 2008. The damage-response framework of microbial
752 pathogenesis and infectious diseases, pp. 135–146. *In*. Springer New York.

753 86. **Casadevall A**, **Pirofski L-a**. 2014. What is a host? Incorporating the microbiota into
754 the damage-response framework **83**:2–7. doi:10.1128/iai.02627-14.

755 87. **Tailford LE**, **Crost EH**, **Kavanaugh D**, **Juge N**. 2015. Mucin glycan foraging in the
756 human gut microbiome. Frontiers in Genetics **6**. doi:10.3389/fgene.2015.00081.

757 88. **Sorg JA**, **Dineen SS**. 2009. Laboratory maintenance ofClostridium difficile. Current
758 Protocols in Microbiology **12**. doi:10.1002/9780471729259.mc09a01s12.

759 89. **Winston JA**, **Thanissery R**, **Montgomery SA**, **Theriot CM**. 2016. Cefoperazone-treated
760 mouse model of clinically-relevant *Clostridium difficile* strain r20291. Journal of Visualized
761 Experiments. doi:10.3791/54850.

762 90. **Kozich JJ**, **Westcott SL**, **Baxter NT**, **Highlander SK**, **Schloss PD**. 2013.
763 Development of a dual-index sequencing strategy and curation pipeline for analyzing
764 amplicon sequence data on the MiSeq illumina sequencing platform. Applied and
765 Environmental Microbiology **79**:5112–5120. doi:10.1128/aem.01043-13.

766 91. **Schloss PD**, **Westcott SL**, **Ryabin T**, **Hall JR**, **Hartmann M**, **Hollister EB**,
767 **Lesniewski RA**, **Oakley BB**, **Parks DH**, **Robinson CJ**, **Sahl JW**, **Stres B**, **Thallinger GG**,
768 **Horn DJV**, **Weber CF**. 2009. Introducing mothur: Open-source, platform-independent,
769 community-supported software for describing and comparing microbial communities.
770 Applied and Environmental Microbiology **75**:7537–7541. doi:10.1128/aem.01541-09.

771 92. **Wang Q**, **Garrity GM**, **Tiedje JM**, **Cole JR**. 2007. Naïve bayesian classifier for
772 rapid assignment of rRNA sequences into the new bacterial taxonomy. Applied and
773 Environmental Microbiology **73**:5261–5267. doi:10.1128/aem.00062-07.

774 93. **Yue JC**, **Clayton MK**. 2005. A similarity measure based on species proportions.
775 Communications in Statistics - Theory and Methods **34**:2123–2131. doi:10.1080/sta-200066418.

776 94. **Segata N**, **Izard J**, **Waldron L**, **Gevers D**, **Miropolsky L**, **Garrett WS**, **Huttenhower**
777 **C**. 2011. Metagenomic biomarker discovery and explanation. Genome Biology **12**:R60.
778 doi:10.1186/gb-2011-12-6-r60.

779 95. **Benjamini Y**, **Hochberg Y**. 1995. Controlling the false discovery rate: A practical and
780 powerful approach to multiple testing. Journal of the Royal Statistical Society: Series B
781 (Methodological) **57**:289–300. doi:10.1111/j.2517-6161.1995.tb02031.x.

782 96. **Topçuoğlu B**, **Lapp Z**, **Sovacool K**, **Snitkin E**, **Wiens J**, **Schloss P**. 2021. Mikropml:
783 User-friendly r package for supervised machine learning pipelines. Journal of Open Source
784 Software **6**:3073. doi:10.21105/joss.03073.

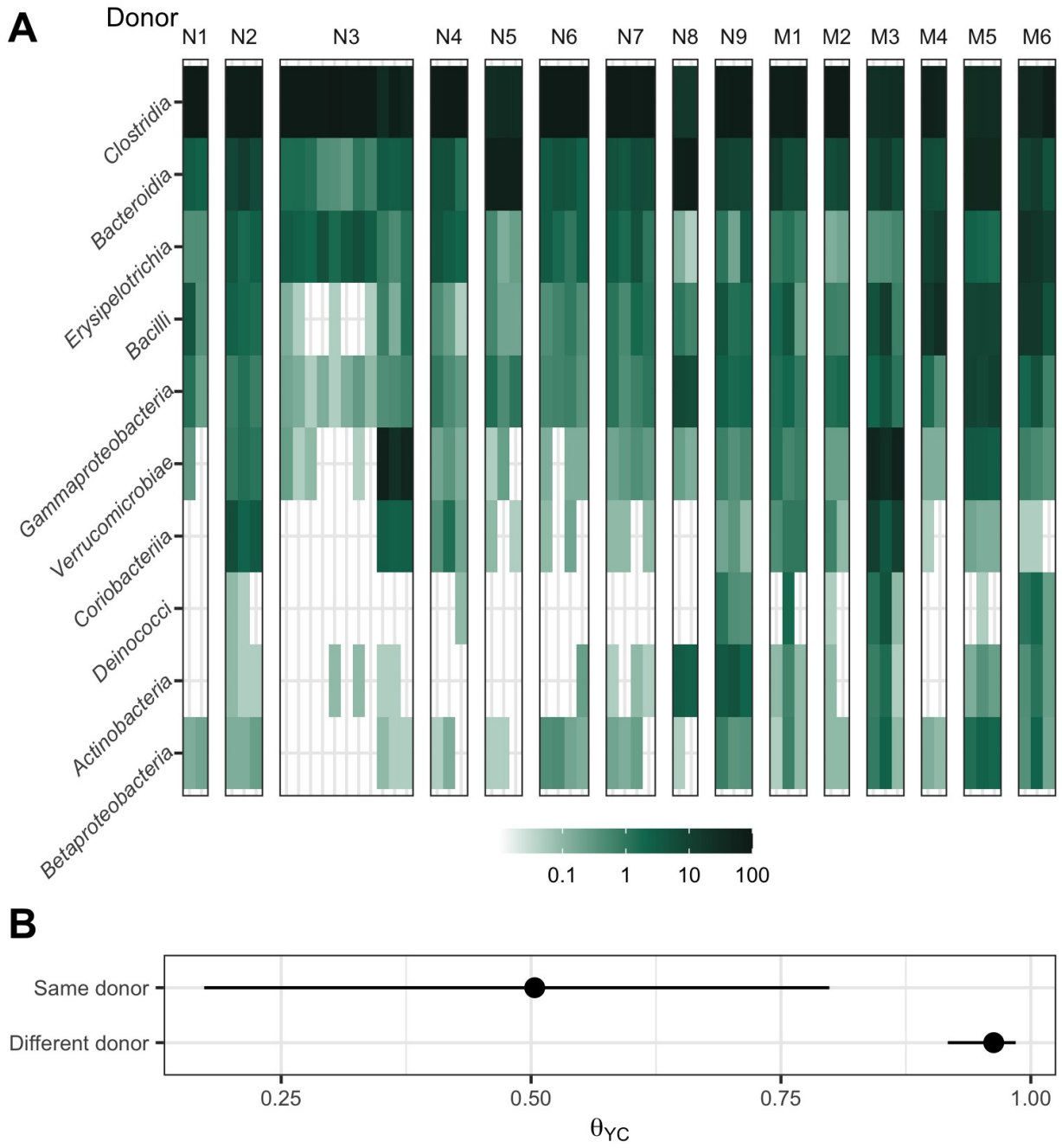

785

786 **Figure 1. Human fecal microbial communities established diverse gut bacterial**
787 **communties in germ-free mice.** (A) Relative abundance of 10 most abundant bacterial
788 classes of the gut bacterial communities on timepoint day 0, 14 days post-colonization
789 of germ-free C57Bl/6 mice with human fecal samples. Each column of abundances
790 represents an individual mouse. Each group of mice that received the same donor are

grouped together and labeled with a letter (N for non-moribund mice and M for moribund mice) and number. (B) Median (points) and interquartile range (lines) of β-diversity (θ_{YC}) between an individual mouse and either all others which were inoculated with feces from the same donor or from a different donor. The β-diversity amongst in the same donor comparison group was significantly less than the β-diversity of the different donor group (*P* < 0.05, calculated by Wilcoxon rank sum test).

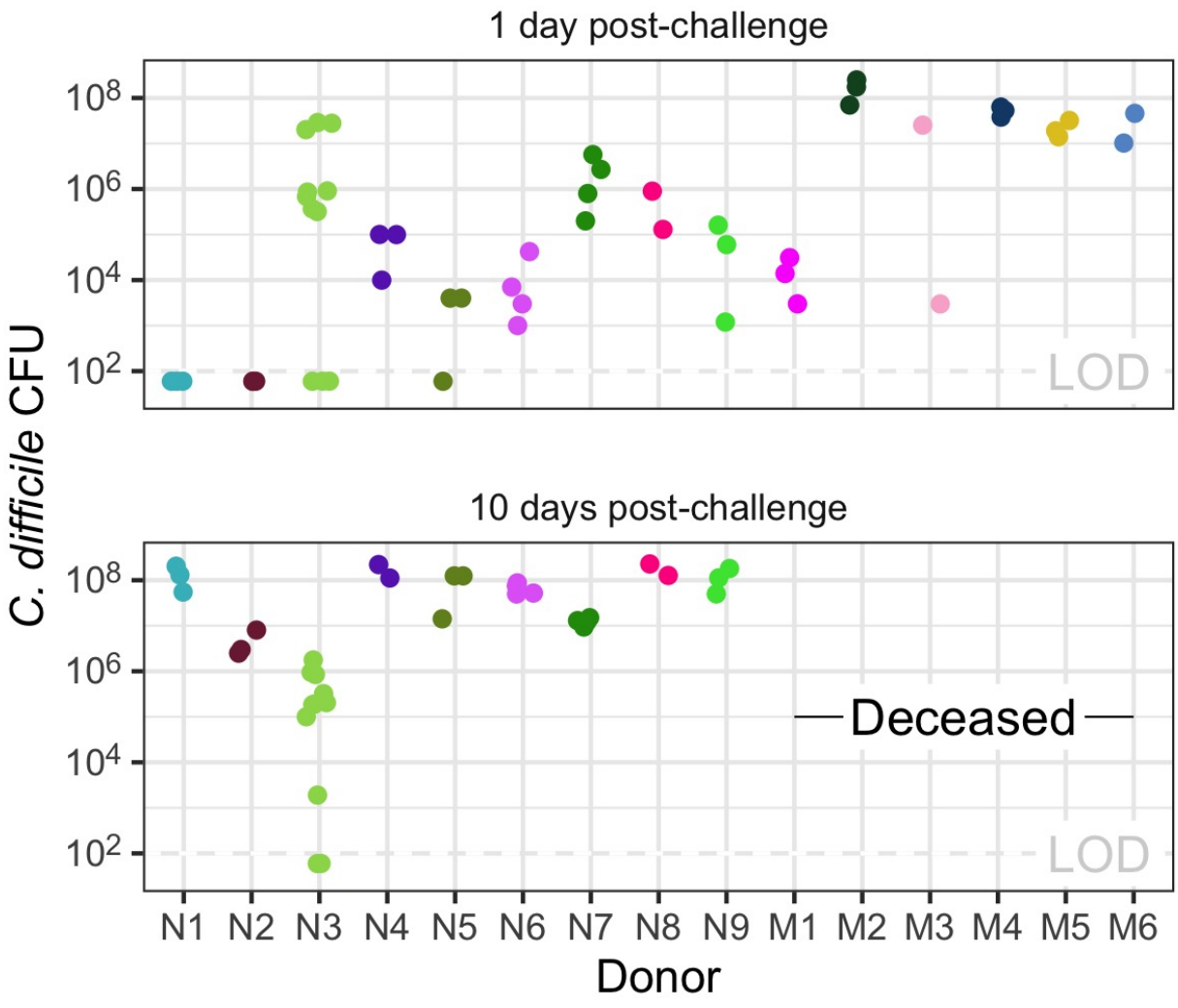

Figure 2. All donor groups resulted in *C. difficile* infection but with different outcomes. *C. difficile* CFU per gram of stool was measured the day after challenge with 10^3 *C. difficile* ribotype 027 human isolate 431 spores and at the end of the experiment, 10 days post-challenge. Each point is an individual mouse. Mice are grouped by donor and labeled by the donor letter (N for non-moribund mice and M for moribund mice) and number. Points are colored by donor group. Mice from donor groups N1 through N6 succumbed to the infection prior to day 10 and were not plated on day 10 post-challenge. LOD = Limit of detection.

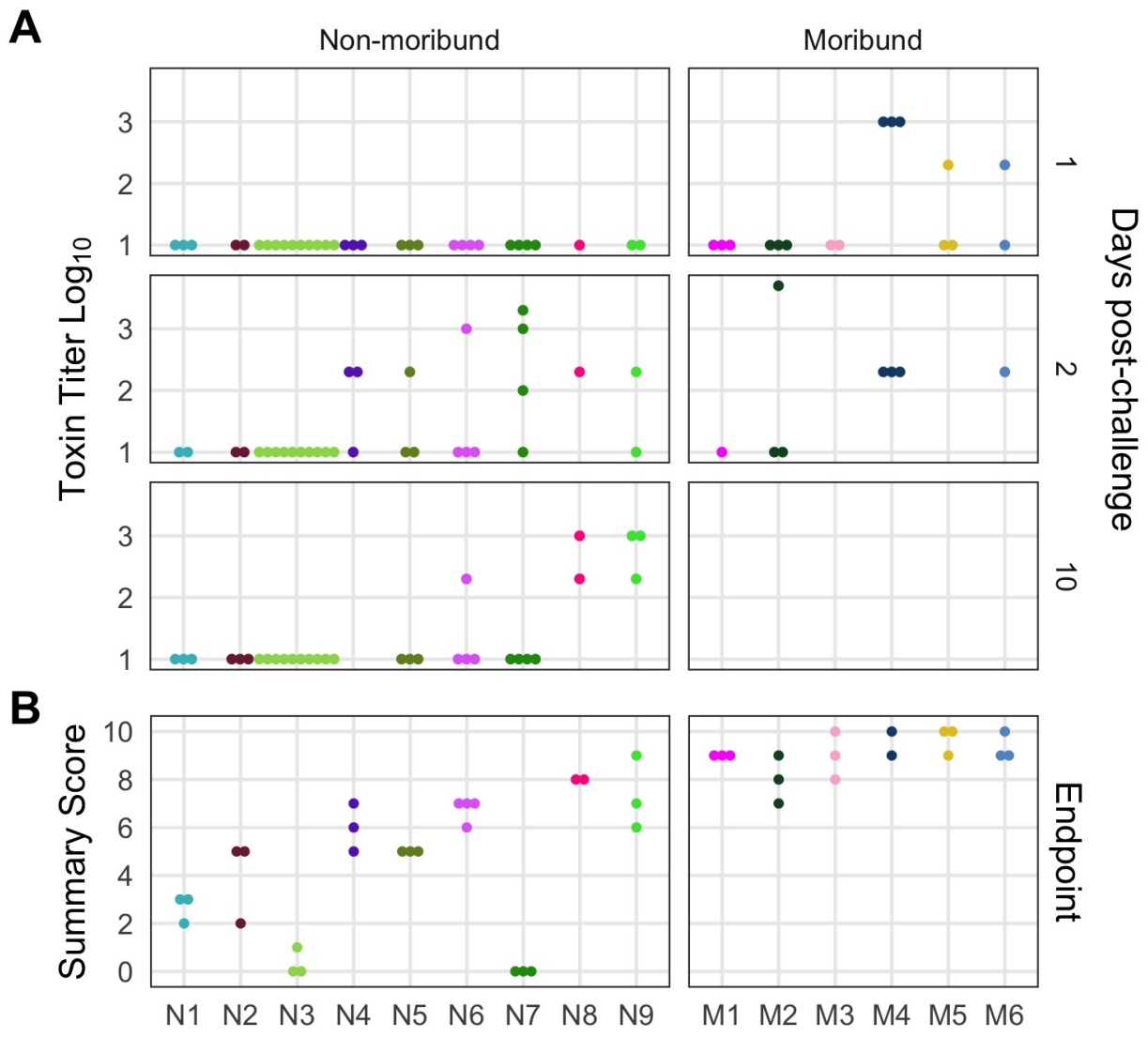

Figure 3. Histopathologic score and toxin activity varied across donor groups. (A) Fecal toxin activity was detected in some mice post *C. difficile challenge in both moribund and non-moribund mice. (B) Cecum scored for histopathologic damage from mice at the end of the experiment. Samples were collected for histopathologic scoring on day 10 post-challenge for non-moribund mice or the day the mouse succumbed to the infection for the moribund group (day 2-3 post-challenge). Each point is an individual mouse. Mice are grouped by donor and labeled by the donor letter (N for non-moribund mice and M for moribund mice) and number. Points are colored by donor group. Missing points are from

819 mice that had insufficient sample collected for assaying fecal toxin.

820

821

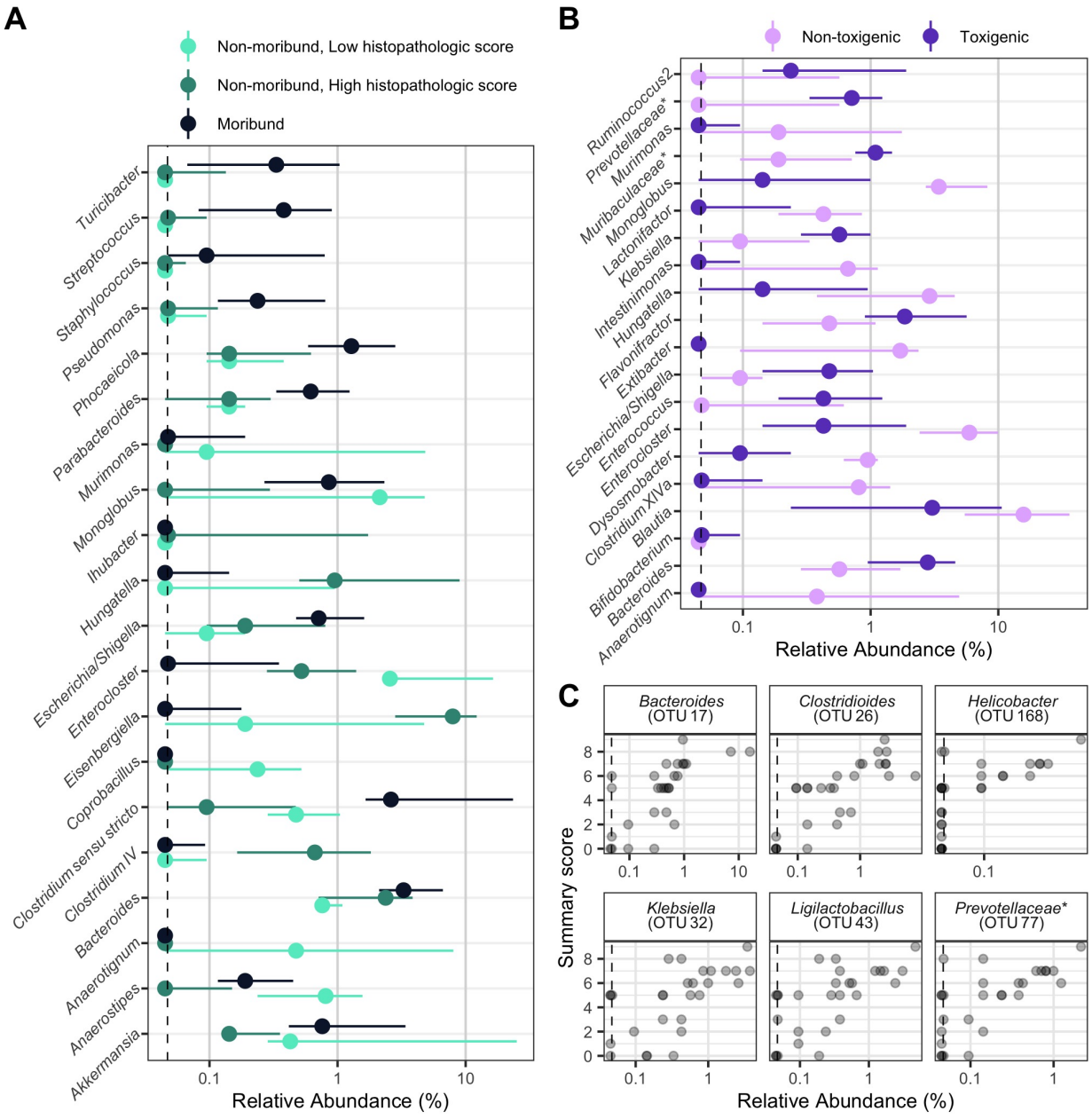

822

823 **Figure 4. Individual fecal bacterial community members of the murine gut associated**

824 **with *C .difficile* infection outcomes.** (A and B) Relative abundance of genera at the

825 time of *C. difficile* challenge (Day 0) that varied significantly by the moribundity and

histopathologic summary score or toxin activity by LEfSe analysis. Median (points) and interquartile range (lines) are plotted. Genera are ordered alphabetically to ease comparisons across analyses. (A) Relative abundances were compared across infection outcome of moribund (colored black) or non-moribund with either a high histopathologic score (score greater than the median score of 5, colored green) or a low histopathologic summary score (score less than the median score of 5, colored light green). (B) Relative abundances were compared between mice which toxin activity was detected (Toxigenic, colored dark purple) and which no toxin activity was detected (Non-toxigenic, colored light purple). (C) Endpoint bacterial OTUs correlated with histopathologic summary score. Each individual mouse is plotted (transparent gray point). Spearman correlations were statistically significant after Benjamini-Hochberg correction for multiple comparisons. * indicates bacterial group was unclassified at lower classification ranks.

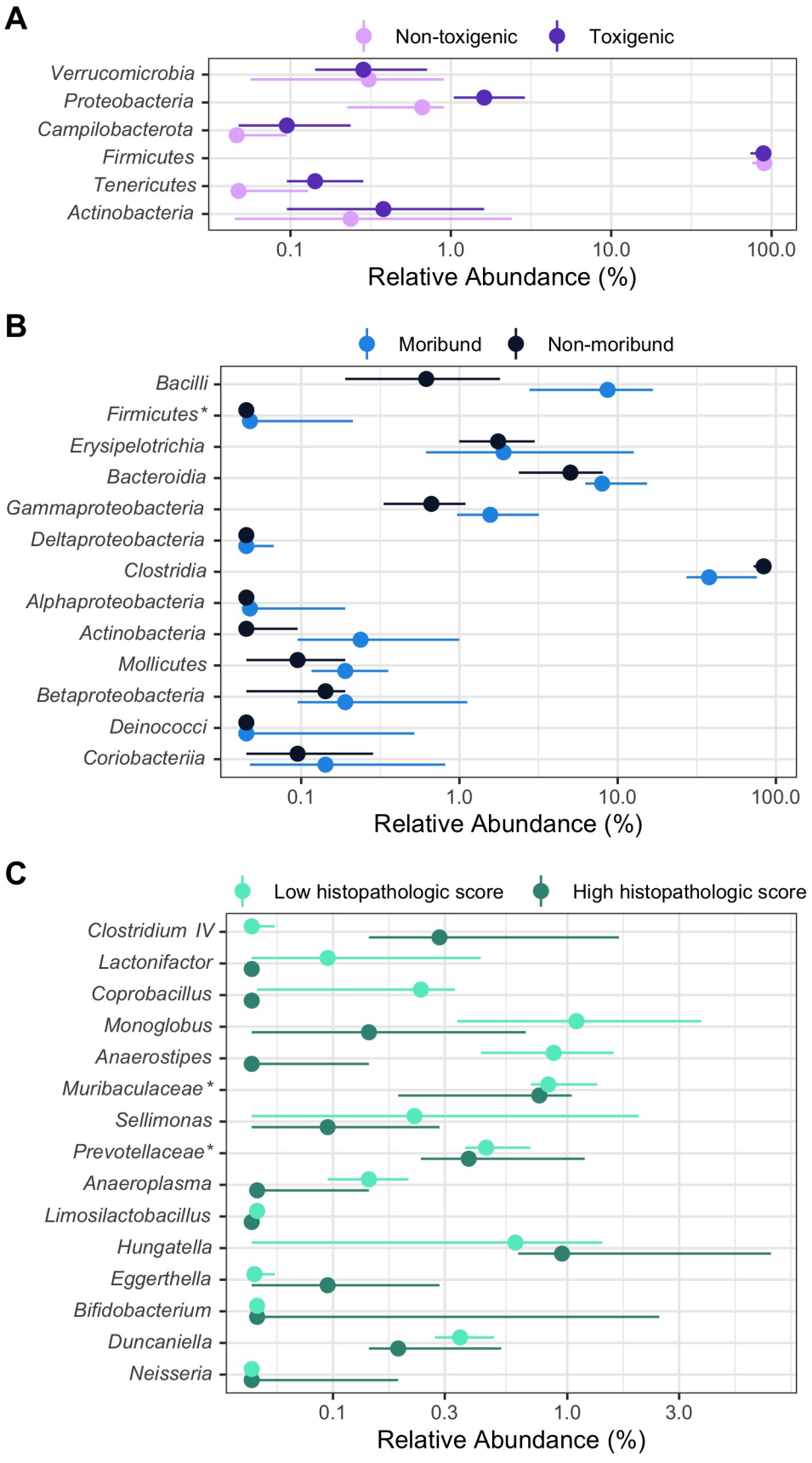
A
Non-toxigenic
Toxigenic
Verrucomicrobia
Proteobacteria
Campilobacterota
Firmicutes
Tenericutes
Actinobacteria
0.1
1.0
10.0
100.0
Relative Abundance (%)
B
Moribund
Non-moribund
Bacilli
Firmicutes*
Erysipelotrichia
Bacteroidia
Gammaproteobacteria
Deltaproteobacteria
Clostridia
Alphaproteobacteria
Actinobacteria
Mollicutes
Betaproteobacteria
Deinococci
Coriobacteriia
0.1
1.0
10.0
100.0
Relative Abundance (%)
C
Low histopathologic score
High histopathologic score
Clostridium IV
Lactonifactor
Coprobacillus
Monoglobus
Anaerostipes
Muribaculaceae*
Sellimonas
Prevotellaceae*
Anaeroplasma
Limosilactobacillus
Hungatella
Eggerthella
Bifidobacterium
Duncaniella
Neisseria
0.1
0.3
1.0
3.0
Relative Abundance (%)

840

Figure 5. Fecal bacterial community members of the murine gut at the time of *C. difficile* (Day 0) predicted outcomes of the infection. Day 0 bacterial community members grouped by different classification rank were modeled with random forest to predict the infection outcome. The models used the highest taxonomic classification rank that performed as well as the lower ranks. Median (solid points) and interquartile range (lines) of the group relative abundance are plotted. Bacterial groups are ordered by their importance to the model; taxonomic group at the top of the plot had the greatest decrease in performance when its relative abundances were permuted. * indicates bacterial group was unclassified at lower classification ranks. (A) Bacterial members grouped by phyla predicted which mice would have toxin activity detected at any point throughout the infection (Toxigenic, dark purple). (B) Bacterial members grouped by class predicted which mice would become moribund (dark blue). (C) Bacterial members grouped by genera predicted if the mice would have a high (score greater than the median score of 5, colored dark green) or low (score less than the median score of 5, colored light green) histopathologic summary score.

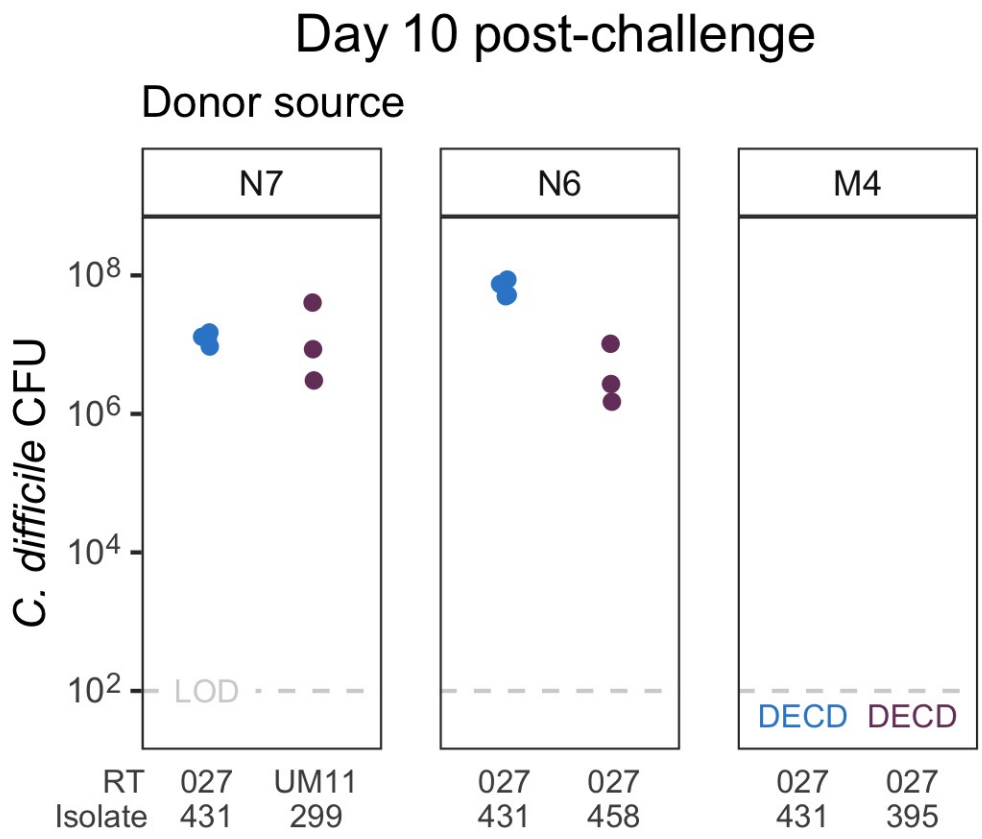
Day 10 post-challenge
Donor source
N7
N6
M4
C. difficile CFU
10^8
10^6
10^4
10^2
LOD
DECD
DECD
RT 027 UM11 027 027 027 027
Isolate 431 299 431 458 431 395

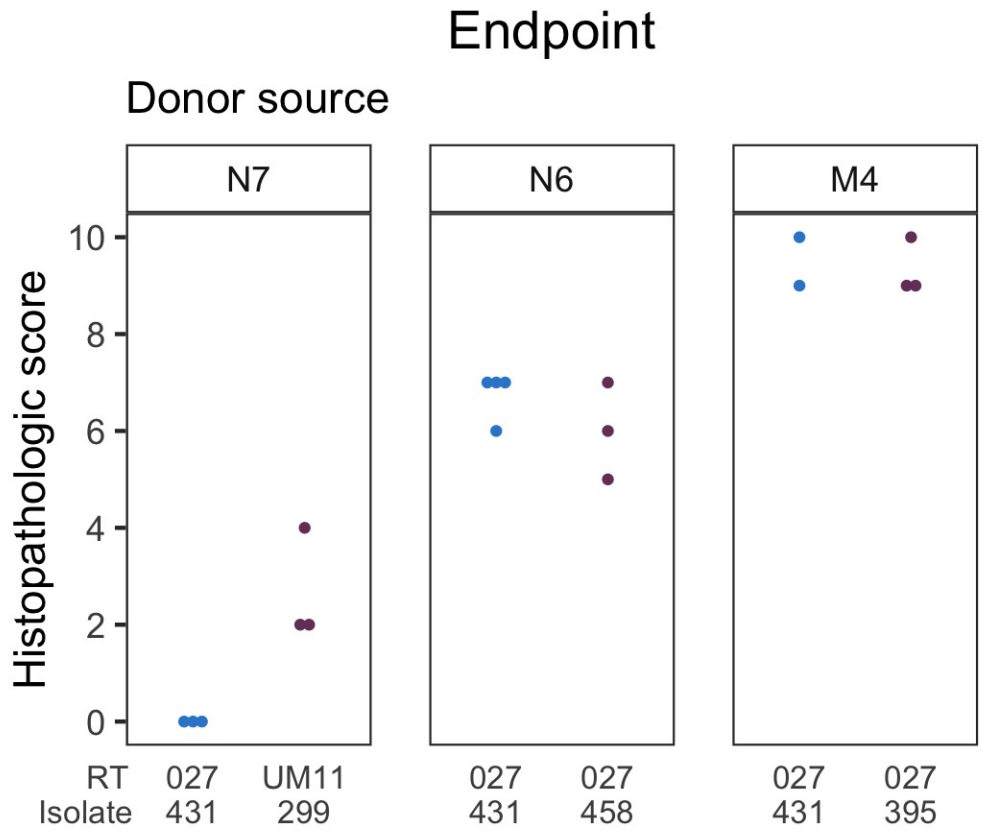
Endpoint
Donor source
N7
N6
M4
Histopathologic score
10
8
6
4
2
0
RT 027 UM11 027 027 027 027
Isolate 431 299 431 458 431 395

858

Figure 6. *C. difficile* infection outcome were similar within human fecal donor groups across different *C. difficile* isolates. Mice colonized with human fecal donor communities N7, N6, or M4 were challenged with the isolate from the previous experiments in this study, *C. difficile* ribotype 027 human isolate 431 (blue points), or a different *C. difficile* isolate (purple points). *C. difficile* CFUs were enumerated at the end of the experiment (day 10 post-challenge) and are plotted grouped by donor source (top plot). Histopathologic scores from the tissue collected at the endpoint (either day 10 post-challenge or day mice succumbed to infection) are plotted grouped by donor source (bottom plot). Mice that had received fecal communities from human donor M4 succumbed to the infection prior to day 10 post-challenge so were not plated for CFU on day 10 post-challenge (DECD = deceased). RT = ribotype, Isolate = *C. difficile* human isolate id, LOD = limit of detection.

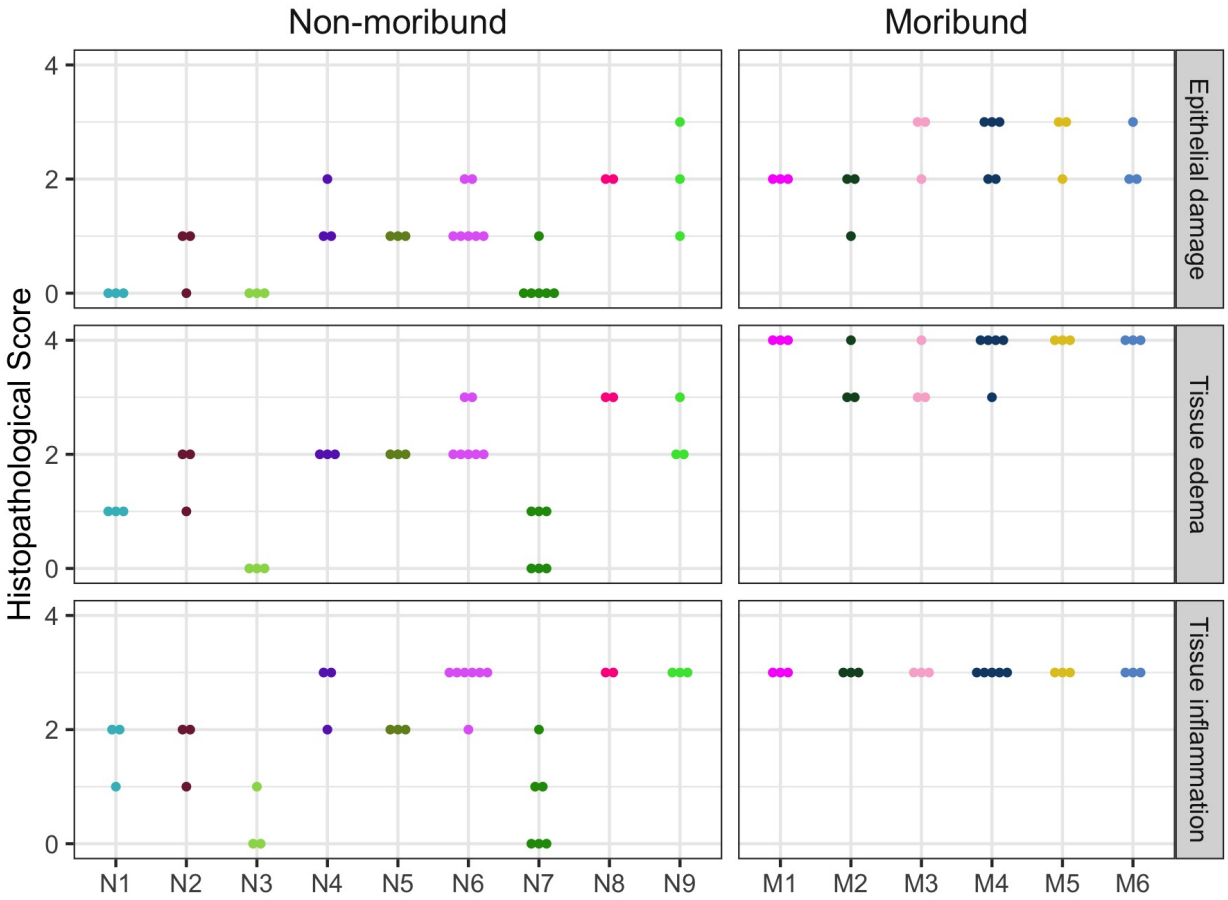

872

873 **Figure S1. Histopathologic score of tissue damage at the endpoint of the infection.**
874 Tissue collected at the endpoint, either day 10 post-challenge (Non-moribund) or day
875 mice succumbed to infection (Moribund), were scored from histopathologic damage. Mice
876 (points) are grouped and colored by their human fecal community donor. Missing points
877 are from mice that had insufficient sample for histopathologic scoring.

878

879

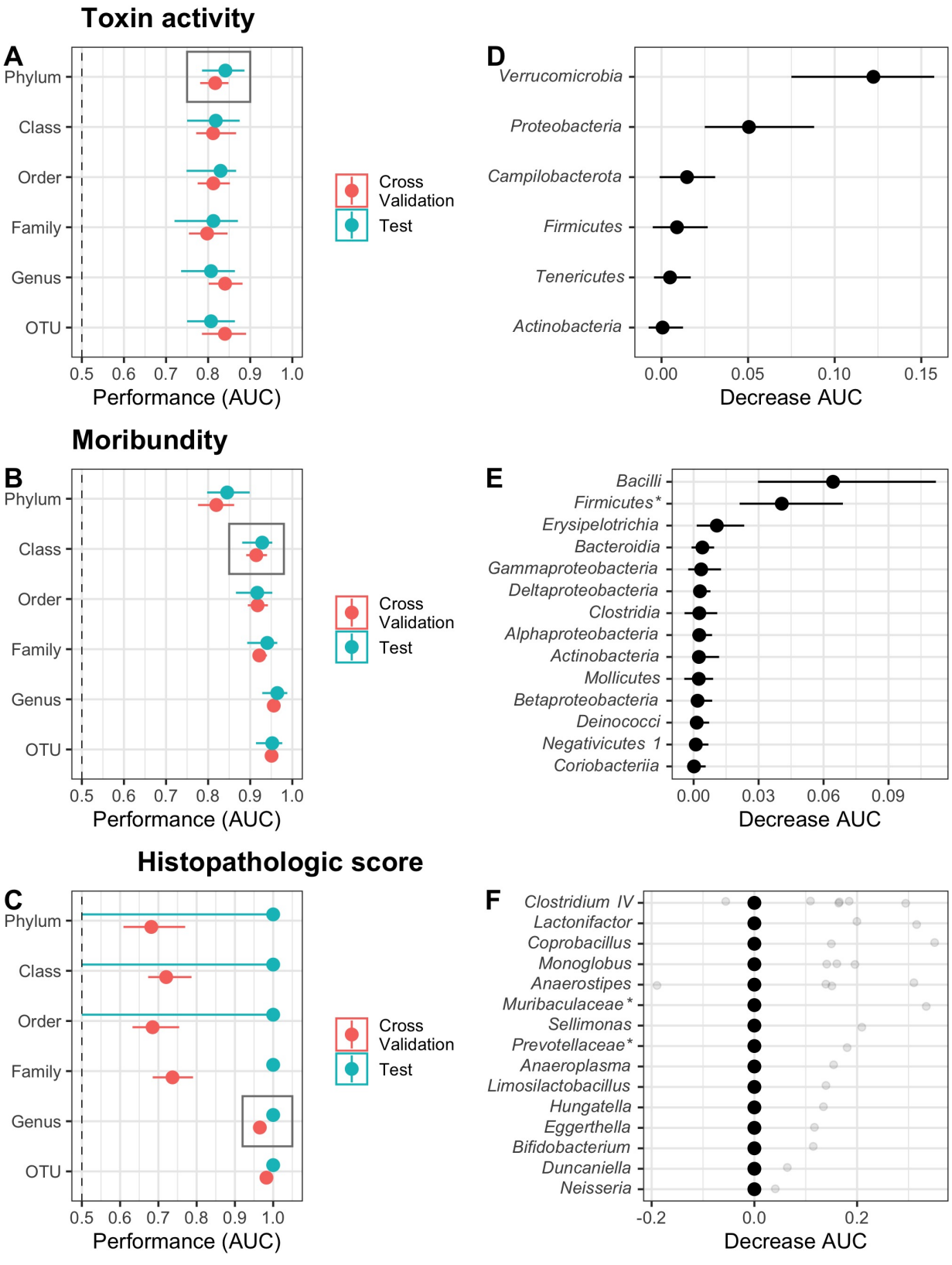
Toxin activity
A
Phylum
Class
Order
Family
Genus
OTU
0.5 0.6 0.7 0.8 0.9 1.0
Performance (AUC)
Cross Validation
Test
D
Verrucomicrobia
Proteobacteria
Campilobacterota
Firmicutes
Tenericutes
Actinobacteria
0.00 0.05 0.10 0.15
Decrease AUC
Moribundity
B
Phylum
Class
Order
Family
Genus
OTU
0.5 0.6 0.7 0.8 0.9 1.0
Performance (AUC)
Cross Validation
Test
E
Bacilli
Firmicutes*
Erysipelotrichia
Bacteroidia
Gammaproteobacteria
Deltaproteobacteria
Clostridia
Alphaproteobacteria
Actinobacteria
Mollicutes
Betaproteobacteria
Deinococci
Negativicutes 1
Coriobacteriia
0.00 0.03 0.06 0.09
Decrease AUC
Histopathologic score
C
Phylum
Class
Order
Family
Genus
OTU
0.5 0.6 0.7 0.8 0.9 1.0
Performance (AUC)
Cross Validation
Test
F
Clostridium IV
Lactonifactor
Coprobacillus
Monoglobus
Anaerostipes
Muribaculaceae*
Sellimonas
Prevotellaceae*
Anaeroplasma
Limosilactobacillus
Hungatella
Eggerthella
Bifidobacterium
Duncaniella
Neisseria
-0.2 0.0 0.2
Decrease AUC

880

Figure S2. Random forest models predicted outcomes of the *C. difficile* challenge. (A-C) Taxonomic classification rank model performance. Relative abundance at the time of *C. difficile* challenge (Day 0) of the bacterial community members grouped by different classification rank were modeled with random forest to predict the infection outcome. The models used the highest taxonomic classification rank that performed as well as the lower ranks. Black rectangle highlights classification rank used to model each outcome. (D-F) Model feature importance. Bacterial groups are ordered by their decrease in area under receiver-operator curve (AUC) when its relative abundances was permuted. Individual relative abundances were added to F since differences in AUC were outside the interquartile range. * indicates bacterial group was unclassified at lower classification ranks. For all plots, median (solid points) and interquartile range (lines) are plotted. (A) Toxin production modeled which mice would have toxin detected during the experiment. (B) Moribundity modeled which mice would succumb to the infection prior to day 10 post-challenge. (C) Histopathologic score modeled which mice would have a high (score greater than the median score of 5) or low (score less than the median score of 5) histopathologic summary score. (D) Bacterial phyla which affected the performance of predicting toxin activity when permuted. (E) Bacterial classes which affected the performance of predicting moribundity when permuted. (D) Bacterial genera which affected the performance of predicting histopathologic score when permuted.

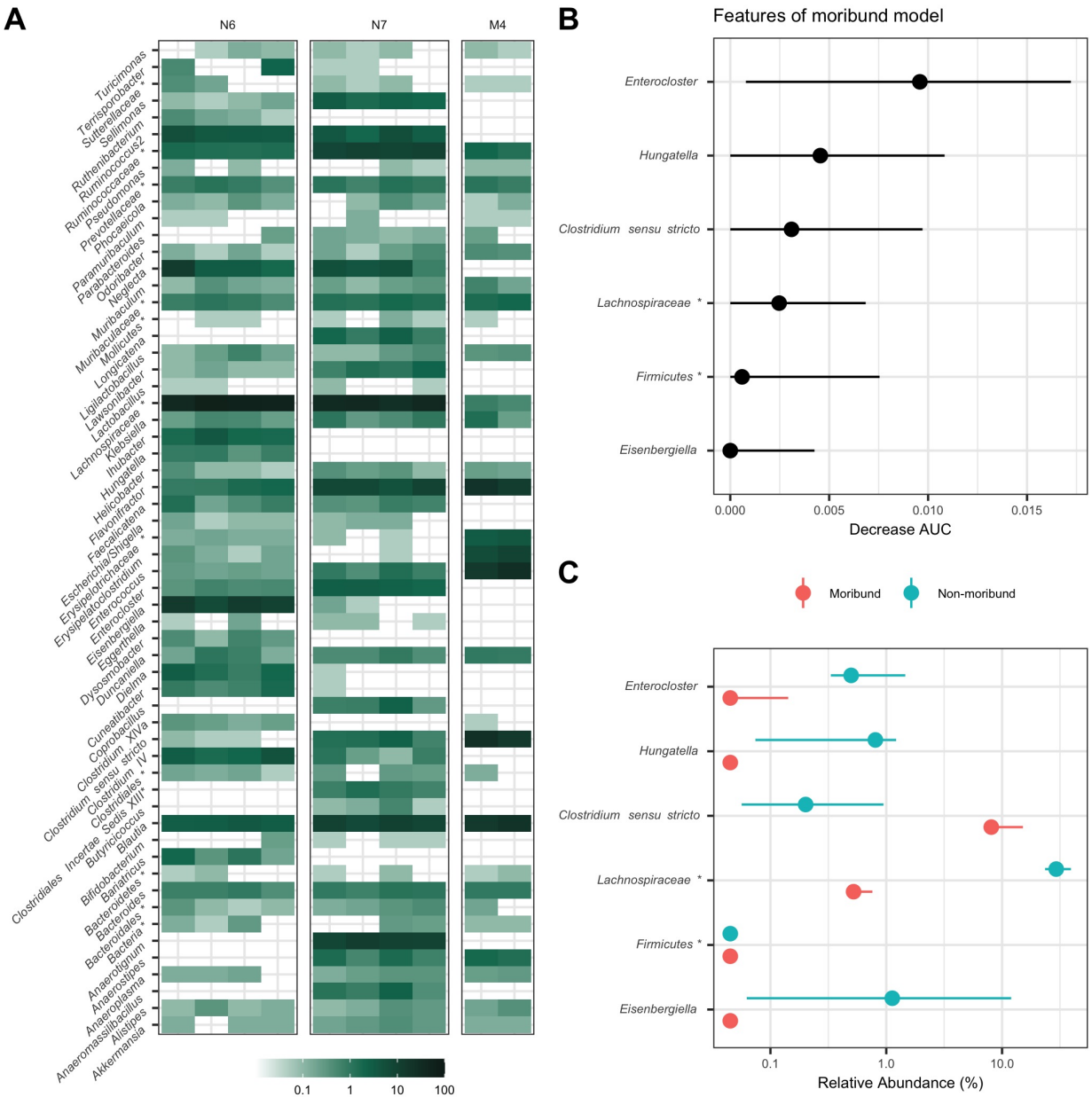

902

903 **Figure S3. Subset of donor communities were selected to test for conserved *C.***
904 ***difficile* infection outcome with a different *C. difficile* isolate.** (A) Relative abundance of
905 genera in mice from previous experiments which received human fecal donor communities
906 N7, N6, or M4. Each column is an individual mouse. (B) Features from the random forest
907 model that predicted moribundity using relative abundance of bacteria were grouped by
908 their genus classification rank and are ordered by their decrease in AUC when each feature
909 was permuted. Median (solid points) and interquartile range (lines) change in AUC are

plotted. (C) Relative abundance of the most important genera used by the model to predict moribundity. Median (solid points) and interquartile range (lines) of the group relative abundances are plotted. * indicates bacterial group was unclassified at lower classification ranks.